Check for updates

JGR Solid Earth

RESEARCH ARTICLE
10.1029/2020JB020040

Along-Margin Variations in Breakup Volcanism at the Eastern North American Margin

John A. Greene[1,2], **Masako Tominaga**[1,3], **and Nathaniel C. Miller**[4]

[1]Department of Geology and Geophysics, Texas A&M University, College Station, TX, USA, [2]Now at Geology Department, Chevron Technical Center, Houston, TX, USA, [3]Department of Geology and Geophysics, Woods Hole Oceanographic Institution, Woods Hole, MA, USA, [4]Woods Hole Coastal and Marine Science Center, United States Geological Survey, Woods Hole, MA, USA

Key Points:
- Variations in the East Coast Magnetic Anomaly indicate coincident variations in the breakup volcanics at the Eastern North American Margin
- Modeling suggests that the East Coast Magnetic Anomaly is produced by first-order (~600–1,000 km) and second-order (~50–100 km) magmatic segmentation
- Second-order magmatic segmentation during breakup likely influenced the segmentation and transform fault spacing of the Mid-Atlantic Ridge

Supporting Information:
- Supporting Information S1

Correspondence to:
J. A. Greene,
greene@tamu.edu

Citation:
Greene, J. A., Tominaga, M., & Miller, N. C. (2020). Along-margin variations in breakup volcanism at the Eastern North American Margin. *Journal of Geophysical Research: Solid Earth*, *125*, e2020JB020040. https://doi.org/10.1029/2020JB020040

Received 1 MAY 2020
Accepted 7 NOV 2020
Accepted article online 16 NOV 2020

©2020. American Geophysical Union. All Rights Reserved.

Abstract We model the magnetic signature of rift-related volcanism to understand the distribution and volume of magmatic activity that occurred during the breakup of Pangaea and early Atlantic opening at the Eastern North American Margin (ENAM). Along-strike variations in the amplitude and character of the prominent East Coast Magnetic Anomaly (ECMA) suggest that the emplacement of the volcanic layers producing this anomaly similarly varied along the margin. We use three-dimensional magnetic forward modeling constrained by seismic interpretations to identify along-margin variations in volcanic thickness and width that can explain the observed amplitude and character of the ECMA. Our model results suggest that the ECMA is produced by a combination of both first-order (~600–1,000 km) and second-order (~50–100 km) magmatic segmentation. The first-order magmatic segmentation could have resulted from preexisting variations in crustal thickness and rheology developed during the tectonic amalgamation of Pangaea. The second-order magmatic segmentation developed during continental breakup and likely influenced the segmentation and transform fault spacing of the initial, and modern, Mid-Atlantic Ridge. These variations in magmatism show how extension and thermal weakening was distributed at the ENAM during continental breakup and how this breakup magmatism was related to both previous and subsequent Wilson cycle stages.

1. Introduction

The cyclic amalgamation and breakup of (super)continents during Wilson cycles are responsible for the configuration and evolution of Earth's surface through time (Wilson, 1966). Continental rifting can be associated with extensive magmatism, and the presence of this magmatism can allow for continental breakup to occur at considerably lower stress by accommodating extension and thermally weakening the plate (Bialas et al., 2010; Buck, 2004, 2006; Daniels et al., 2014; Ebinger & Casey, 2001; Kendall et al., 2005). Localized magmatism at the site of eventual continental breakup produces a thick wedge of volcanic layers that is a characteristic feature observed at magma-rich rifted continental margins worldwide (e.g., Hinz, 1981; Morgan & Watts, 2018; Mutter, 1985). As these margins cooled, these volcanic layers subsided, producing the seaward-dipping reflectors (SDRs) observed in seismic images of rifted margins (e.g., White & McKenzie, 1989). Understanding continental breakup is significant due to its impact on Earth's climate and mass extinction events (Donnadieu et al., 2006; Nomade et al., 2007; Simms & Ruffell, 1989). The architecture of the ensuing rifted continental margin is governed by the rifting and breakup history and influences the prevalence of both natural resources (Mann et al., 2003; Nelson et al., 1992) and geohazards (e.g., rifted margin seismicity, submarine landslides, and tsunamis) (Brune, 2016; Chaytor et al., 2009).

The Eastern North American Margin (ENAM) (Figures 1 and 2) records the beginning of the current Wilson cycle, which initiated with the breakup of the supercontinent Pangaea and continues with the ongoing formation of the Atlantic Ocean (Thomas, 2019; Wilson, 1966). The ENAM is a prime location for understanding the processes involved in the formation and evolution of rifted continental margins (Lynner et al., 2020; Sheridan, 1989; Withjack et al., 1998). The prominent East Coast Magnetic Anomaly (ECMA) extending along the ENAM (Figure 1a) is commonly attributed to the volcanics emplaced as the surficial component of the magmatism at the site of eventual continental breakup (Austin et al., 1990; Davis et al., 2018; Talwani et al., 1995). Along-strike variation in the ECMA amplitude and character (Figure 1b) suggests

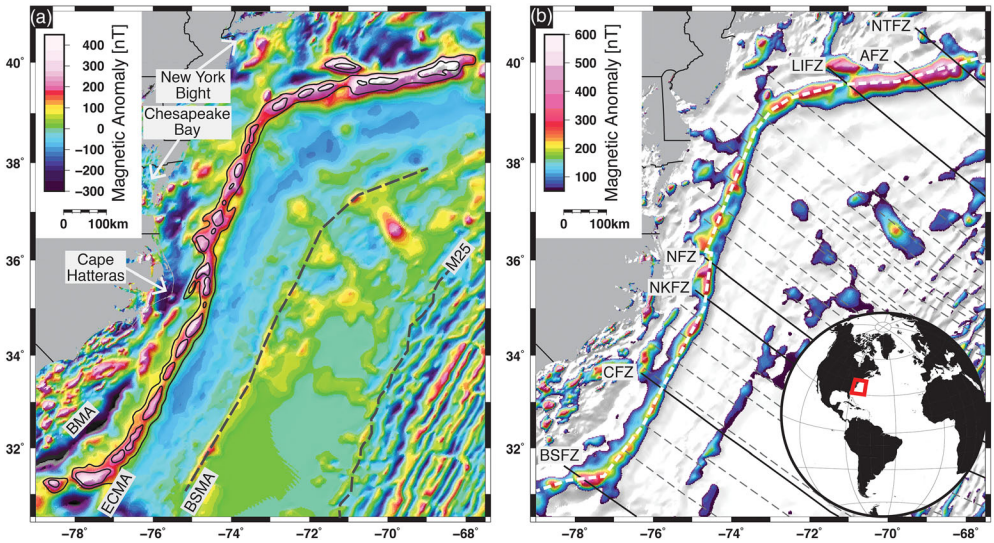

Figure 1. (a) North American Magnetic Anomaly Group (NAMAG) compilation magnetic anomaly grid (Bankey et al., 2002). Extent of ECMA shown with dark contours (Klitgord et al., 1988). Gray lines identify the BSMA and anomaly M25 (Greene et al., 2017). (b) Magnetic anomaly grid with scale adjusted to highlight ECMA amplitude variation. Black lines show landward extrapolations of major (solid) and minor (dashed) fracture zones for the Atlantic, with Blake Spur (BSFZ), Carolinas (CFZ), Northern Kane (NKFZ), Norfolk (NFZ), Long Island (LIFZ), Atlantis (AFZ), and Nantucket (NTFZ) Fracture Zones labeled (Klitgord et al., 1988). White dashed line shows profile for along-margin extractions of data and model results (Figure 4).

that the amount and distribution of breakup magmatism at the ENAM likewise varied along the margin (e.g., Behn & Lin, 2000). Rifting is a three-dimensional process, and identifying how the amount and distribution of magmatism varies along the margin, along with the associated extension accommodation and thermal weakening (e.g., Kendall et al., 2005), is important for understanding the entire breakup process at rifted continental margins like the ENAM. The amount, distribution, and causes of breakup magmatism at the ENAM have not been extensively investigated in a full, along margin framework.

Magmatic segmentation and transform fault locations along seafloor spreading centers may be inherited from both preexisting structure in the continental lithosphere and the continental breakup process (e.g., Behn & Lin, 2000; Bellahsen et al., 2013; Beutel et al., 2010; Collier et al., 2017; Hammond et al., 2013;

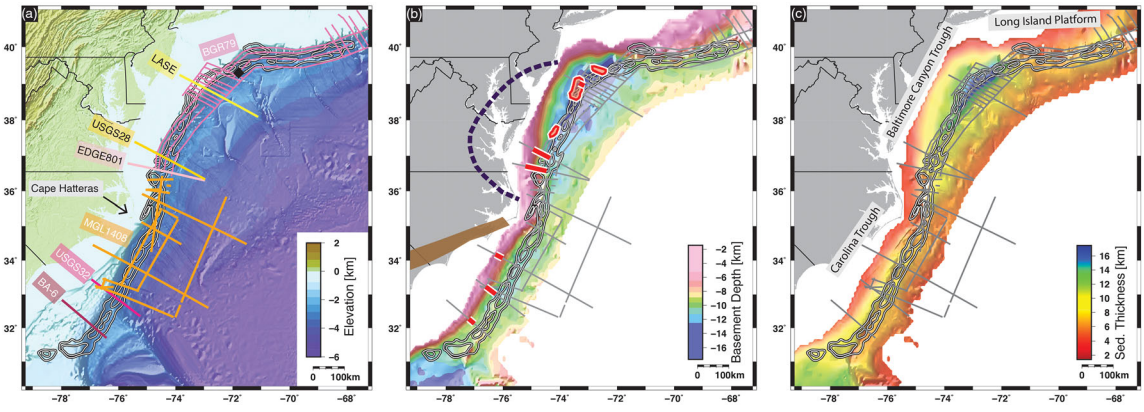

Figure 2. (a) ETOPO1 bathymetry (Amante & Eakins, 2009), (b) seismically derived basement depth (Hutchinson et al., 1995; Klitgord et al., 1994), and (c) sediment thickness. ECMA extent indicated by black/white contours (Figure 1a) (Klitgord et al., 1988). Key seismic lines/surveys labeled; red lines/polygons indicate extent of SDR interpretations from previous studies (Austin et al., 1990; Bécel et al., 2020; Hinz, 1981; Holbrook et al., 1994; LASE Study Group, 1986; Sheridan et al., 1993; Tréhu et al., 1989). Purple dashed line indicates the inferred suture zone surrounding a hypothesized isolated piece of West African Craton under Chesapeake Bay (Lefort & Max, 1991, their Figure 7). Brown polygon indicates the inferred location of the Alleghanian suture zone separating pre-Alleghanian Laurentian terranes (to the north) from the Gondwanan terranes (to the south) (Boote & Knapp, 2016; Higgins & Zietz, 1983). Black diamond indicates location of heat flow Site V20-232 (Pollack et al., 1993).

Hayward & Ebinger, 1996; Keranen et al., 2004). Structural elements (e.g., zones of weakness and crustal thickness) developed during previous Wilson cycles can be transferred to the mid-ocean ridge during rifting and breakup and further mid-ocean ridge segmentation may develop from the magmatic segmentation during breakup, suggesting that consistent elements persist through time as (super)continents amalgamate and breakup (Bellahsen et al., 2013; Franke et al., 2007; Hayward & Ebinger, 1996). A relationship between breakup and seafloor spreading segmentation has been suggested for the ENAM based on the similarity of the potential field anomaly wavelengths along the margin and modern Mid-Atlantic Ridge (e.g., Behn & Lin, 2000). However, how the three-dimensional distribution of breakup magmatism at the ENAM corresponds with the Mid-Atlantic Ridge magmatic segmentation following breakup has not been comprehensibly examined to understand the possible genetic relationship between preexisting structure, magmatic emplacement during rifting, and the magmatic segmentation of mid-ocean ridges.

In this study, we investigate along-margin variations in the thickness and width of the breakup volcanic wedge at the ENAM. While numerous styles of magmatism and tectonics can be present at rifts throughout their history (Geoffroy et al., 2015; Marzoli et al., 2018; Menzies et al., 2002), we focus this study on the volcanic wedge emplaced during final continental breakup, which can be analyzed using magnetic data. This volcanic wedge serves as the extrusive component of the focused magmatism that accommodated continental breakup and the transition to seafloor spreading (Holbrook & Kelemen, 1993; Withjack et al., 2012). We use magnetic modeling, leveraging the extensive, and continuous, coverage of magnetic anomaly data available at the ENAM (Figure 1) (Bankey et al., 2002) to address: (1) Does the variation in the ECMA amplitude and character indicate along-strike variations in the amount and distribution of breakup magmatism, (2) what are the possible causes of magmatic segmentation at the ENAM during breakup, and (3) did breakup magmatism influence the segmentation of the Mid-Atlantic Ridge. Other geophysical data, such as seismic, are sparsely distributed over the ENAM (Figure 2) and have difficultly continuously imaging deep margin structure. Nevertheless, we use such information to augment and constrain for our magnetic modeling results wherever they are available at the ENAM (Figure 2) (Austin et al., 1990; Bécel et al., 2020; Hinz, 1981; Holbrook et al., 1994; Lase Study Group, 1986; Sheridan et al., 1993; Talwani et al., 1995; Tréhu et al., 1989). Based on our magnetic modeling, we show that the observed variations in the ECMA amplitude and character can be explained by first- and second-order along-strike variations in the thickness and width of breakup volcanism, which provide new insights into the distribution and amount of magmatism at the ENAM.

2. Background

2.1. Continental Rifting and Breakup

The continental rifting and breakup stage of Wilson cycles (Wilson, 1966) results in the formation of rifted continental margins and the initiation of seafloor spreading that produces ocean basins (Brune, 2016; Ebinger, 2005). Rifted continental margins total ~105,000 km in length globally and record the history of continental rifting/breakup and the postrift evolution of these settings (Bradley, 2008; Brune, 2016). Continental rifting is active in the East African Rift (Ebinger & Casey, 2001; Makris & Ginzburg, 1987) and Afar (Manighetti et al., 1997, 1998), and the transition to seafloor spreading is ongoing or has recently occurred in the Red Sea (Almalki et al., 2015; Lowell & Genik, 1972), the Eastern Black Sea (Monteleone et al., 2019), and the Gulf of California (Lizarralde et al., 2007).

Rifted margins fall on a spectrum between two end-member types, magma rich and magma poor, based on the amount of magma present during breakup (Franke, 2013; Gallahue et al., 2020; Geoffroy, 2005; Geoffroy et al., 2015; Menzies et al., 2002; Péron-Pinvidic et al., 2013; Tugend et al., 2018). At magma-rich rifted margins, voluminous intrusive and extrusive magmatic activity facilitates and results from continental rifting and breakup, as this magmatism can thermally weakening the plate, localize strain, and accommodate extension to allow continental breakup at a lower stress (Bastow & Keir, 2011; Bialas et al., 2010; Buck, 2004; Daniels et al., 2014; Ebinger & Casey, 2001). Flood basalts are generally emplaced during the prerift and/or synrift stages of rifting (Marzoli et al., 2018; Menzies et al., 2002). Additionally, focused magmatism expressed as volcanic flows, mafic intrusions, and/or igneous underplating occurs during continental breakup and the transition to seafloor spreading (Bastow & Keir, 2011; Geoffroy et al., 2015; White et al., 1987). In contrast, magma-poor rifted margins typically exhibit some combination of extreme

crustal thinning, detachment faulting, and/or mantle exhumation during rifting and breakup (Boillot et al., 1980; Franke, 2013).

A wedge-shaped accumulation of volcanics is emplaced along magma-rich margins as the extrusive portion of breakup magmatism (Mutter, 1985; White et al., 1987). This volcanic wedge is imaged as SDRs in seismic data at magma-rich rifted margins around the world (e.g., Austin et al., 1990; Eldholm et al., 2000; Gallahue et al., 2020; Hinz, 1981; Morgan & Watts, 2018; Mutter, 1985; Mutter et al., 1982; Oh et al., 1995; White & McKenzie, 1989). Horizontal volcanic flows are erupted subaerially before acquiring a seaward dip from either magmatic loading and thermal subsidence of the lithosphere or slip along bounding normal faults (Buck, 2017; Morgan & Watts, 2018). The volcanic wedge is associated with and likely responsible for a high-amplitude, margin parallel magnetic anomaly (e.g., Berndt et al., 2001; Collier et al., 2017; Corner et al., 2002; Davis et al., 2018; Franke et al., 2019; Keen & Potter, 1995). The presence of breakup volcanic wedges has been confirmed by drilling at the Greenland and Norwegian margins (e.g., Eldholm et al., 1989; Vandamme & Ali, 1998), and analogous volcanic flows exist at modern rift sites, such as the Afar region of Ethiopia (e.g., Bastow & Keir, 2011; Beutel et al., 2010; Keir et al., 2013). Beneath the SDRs, high-velocity lower crust is often observed in seismic data, interpreted to represent mafic intrusives and/or underplating during breakup (Holbrook et al., 1994; Kelemen & Holbrook, 1995; Mjelde et al., 2016; Talwani & Abreu, 2000; Tréhu et al., 1989; White et al., 1987, 2008).

Magma-rich rifted continental margins are prevalent worldwide (Gallahue et al., 2020; Hinz, 1981; Menzies et al., 2002). Rifted margins that are thought to be closer to the magma-rich end-member of the spectrum include the ENAM in the Central Atlantic (e.g., Austin et al., 1990; Holbrook & Kelemen, 1993), portions of the conjugate margins of the South Atlantic (e.g., Franke et al., 2007; Koopmann et al., 2014) and North Atlantic (e.g., Eldholm & Grue, 1994; Mutter et al., 1982), the margin of the Canadian Arctic (Funck et al., 2011), the margin of East Antarctica (Gupta et al., 2017), the Northwestern Australian Margin (e.g., Hopper et al., 1992), and the Southwest Indian Margin (e.g., Ajay et al., 2010). Magma-poor margins include the conjugate Newfoundland, Canada, and Iberia Peninsula margins (e.g., Boillot et al., 1980; Shillington et al., 2006; Whitmarsh et al., 2001) and the Gulf of Aden (Autin et al., 2010; d'Acremont et al., 2005). Intermediate examples, with elements of both end-members, include the South China Sea (e.g., Franke, 2013; Weiwei et al., 2012) and the Gulf of California (Lizarralde et al., 2007).

Along-axis magmatic segmentation is a feature of both presently active rifts (e.g., Beutel et al., 2010; Hammond et al., 2013; Hayward & Ebinger, 1996; Keir et al., 2013; Manighetti et al., 1998, 2001) and magma-rich rifted continental margins (Collier et al., 2017; Franke et al., 2019; Geoffroy, 2005; Koopmann et al., 2014). The greater amount of magma in the center of these segments is related to along-margin variations in extension during breakup (Ebinger & Casey, 2001; Geoffroy, 2001). Following successful continental breakup, a segmented mid-ocean ridge develops as the tectonic regime enters the seafloor spreading stage (Bellahsen et al., 2013; Ebinger, 2005). The magmatic segmentation currently observed in both rifts and mid-ocean ridges are thought to be caused by (1) along-strike variations in magma production from focused upwelling of warmer asthenospheric mantle initiated by Rayleigh-Taylor gravitational instability (Geoffroy, 2001; Lin et al., 1990; Schouten et al., 1985; Sempéré et al., 1993; Whitehead et al., 1984); (2) magma focusing from melt transport at the base of the lithosphere (e.g., Keir et al., 2015; Magde & Sparks, 1997; Shillington et al., 2009); or (3) tectonic extension with associated decompression melting and dike intrusion (Ebinger & Casey, 2001; Manighetti et al., 1998, 2001). The length scale of magmatic segmentation is similar in both rifts and the ensuing mid-ocean ridges, which suggests that mid-ocean ridge segmentation is inherited from the magmatic segmentation present during the continental breakup process (e.g., Behn & Lin, 2000; Bellahsen et al., 2013; Beutel et al., 2010; Collier et al., 2017; Hammond et al., 2013; Hayward & Ebinger, 1996; Keranen et al., 2004).

2.2. ENAM Formation

Eastern North America has been the site of repeated iterations of continental amalgamation and breakup through time (Thomas, 2019). A prominent stage in the history of modern-day Eastern North America is the assembly and breakup of the most recent supercontinent, Pangaea (Rankin, 1994). The assembly of Pangaea initiated during the Early and Middle Paleozoic when peri-Gondwanan terranes (such as the Carolina, Avalon, and Gander terranes), present in the oceans separating Laurentia and Gondwana, was accreted onto the eastern margin of the Laurentian landmass (Hatcher, 2010). The amalgamation of

Pangaea culminated with the Late Paleozoic Alleghanian orogeny (320–260 Ma) (Hatcher, 2002). This continental collision created the Alleghanian suture zone, which is now located in North/South Carolina and Georgia to separate the pre-Alleghanian Laurentian terranes (including the peri-Gondwanan Carolina terrane) to the northeast from the accreted (peri-)Gondwanan terranes (e.g., Suwannee and Charleston/Brunswick terranes) to the southwest (Figure 2b) (Boote & Knapp, 2016).

The ENAM (Figure 1) formed from the diachronous breakup of Pangaea, which occurred earlier (earliest Jurassic) off the southeastern United States and later (early Cretaceous) off Canada (Withjack et al., 2012). The southern ENAM (south of Nova Scotia) is thought to be a magma-rich continental margin, whereas the northern ENAM is magma poor (Keen & Potter, 1995; Kelemen & Holbrook, 1995; Shillington et al., 2006). Continental rifting of Pangaea in modern eastern North America initiated in the Late Triassic (Withjack et al., 2012). Northwest-southeast crustal extension was initially accommodated over a broad zone by faults bounding long-lived rift basins (Manspeizer & Cousminer, 1988). Many of these extensional faults were reactivated preexisting Paleozoic structures (Schlische, 1993). During rifting, widespread magmatism and distributed diking associated with the Central Atlantic Magmatic Province (CAMP) was emplaced at ~200 Ma (Blackburn et al., 2013; Marzoli et al., 2018). As rifting progressed, extension was localized at the site of eventual continental breakup and rift basin faulting ceased (Withjack et al., 1998).

At the southern ENAM, continental breakup and the transition to seafloor spreading is thought to have been accommodated by magmatic activity based on multiple geophysical indicators, including SDRs, high-velocity lower crust, and a high-amplitude magnetic anomaly (e.g., Austin et al., 1990; Holbrook et al., 1994; Talwani et al., 1995). SDRs were first identified at the ENAM by Hinz (1981) in seismic reflection data, and they interpreted these SDRs to represent volcanism during continental breakup. Numerous seismic surveys led to further, extensive investigation of SDRs at the ENAM (Figure 2b), providing additional support to the interpretation that the SDRs represent the subaerial emplacement, and subsequent subsidence, of a volcanic wedge along the margin (e.g., Austin et al., 1990; Bécel et al., 2020; Holbrook et al., 1994; Lase Study Group, 1986; Oh et al., 1995; Sheridan et al., 1993; Talwani et al., 1995; Tréhu et al., 1989). SDRs at the ENAM are overlaid by the thick sediment of the Carolina Trough, Baltimore Canyon Trough, and Georges Bank sedimentary basins (Figure 2c) (Klitgord et al., 1988). In the Carolina and Baltimore Canyon troughs, crustal seismic refraction measurements also exist, which are not available in the Georges Bank Basin to the north (Holbrook et al., 1994; Kelemen & Holbrook, 1995; Lase Study Group, 1986; Tréhu et al., 1989). These refraction measurements show that the SDRs are underlain by high-velocity lower crust, interpreted to represent mafic intrusions and/or igneous underplating during breakup (e.g., Kelemen & Holbrook, 1995). Similar indicators of magmatic activity are not readily identifiable on the conjugate Northwest African Margin (Biari et al., 2017; Klingelhoefer et al., 2009; Labails et al., 2009), being limited to a poorly developed SDR package (Roeser et al., 2002). This asymmetry in breakup magmatism between the ENAM and Northwest African Margin may indicate stronger magmatic activity on the ENAM related to the preferential rising of hot mantle material beneath this margin, with magmatic activity on the Northwest African Margin limited to moderate volcanic intrusions (Biari et al., 2017; Klingelhoefer et al., 2009).

The ECMA is a 2,500-km-long, high-amplitude, positive magnetic anomaly extending along the ENAM from offshore Georgia to Nova Scotia (Figure 1) (Klitgord & Schouten, 1986). The ECMA was first identified by Keller et al. (1954) on two aeromagnetic profiles, and was later comprehensively mapped during a U.S. Naval Oceanographic Office aeromagnetic survey (Taylor et al., 1968). After its discovery, various sources for the ECMA were proposed, including a basement ridge (Klitgord & Berhrendt, 1979), an edge effect from the juxtaposition of higher- and lower-magnetized crust (Hutchinson et al., 1982; McBride & Nelson, 1988) or highly magnetized crust (Alsop & Talwani, 1984; Keller et al., 1954; Taylor et al., 1968). Following the identification of SDRs in seismic data that are spatially correlated with the ECMA (e.g., Austin et al., 1990; Holbrook et al., 1994; Lase Study Group, 1986; Sheridan et al., 1993; Tréhu et al., 1989), the general consensus has been that ECMA is attributed to the volcanic wedge emplaced during continental breakup based on the results of 2-D magnetic forward modeling (e.g., Austin et al., 1990; Bécel et al., 2020; Davis et al., 2018; Talwani et al., 1995). Talwani et al. (1995) suggest that the ECMA is a remanent anomaly from a rapidly emplaced volcanic wedge. Alternatively, Davis et al. (2018) suggest that the ECMA is an induced anomaly, with a longer-duration (6–31 Myr) of emplacement over multiple polarity periods causing the remanent magnetization of the volcanic wedge layers to cancel out. To the north, offshore Nova Scotia, the ECMA

diminishes and SDRs are not found, suggesting that the margin transitions to more magma poor at this location (Keen & Potter, 1995; Van Avendonk et al., 2006).

The ECMA displays notable along-strike variations in amplitude and character at multiple scales (Figure 1b) (Behn & Lin, 2000; Klitgord et al., 1988). A regional change in the ECMA character occurs near Cape Hatteras, North Carolina, with the single peak ECMA to the north of Cape Hatteras and a comparatively lower amplitude, broader ECMA with two peaks to the south (Figure 1) (Klitgord et al., 1988). A change in ECMA amplitude is present offshore the New York Bight, being higher to the northeast in the Long Island Platform and comparatively lower to the south in the Baltimore Canyon and Carolina troughs (Figure 1). The ECMA also displays amplitude variation at a 100- to 150-km wavelength, with magnetic anomaly highs separated by zones of relatively lower amplitude (Figure 1b) (Behn & Lin, 2000).

The ENAM also contains another prominent magnetic anomaly, the Brunswick Magnetic Anomaly (BMA), which is located inboard and parallel to the ECMA in the Carolina Trough (Klitgord et al., 1988) (Figure 1). The source of the BMA is debated but is thought to play a role in the ENAM rift history (Duff & Kellogg, 2019). Proposed sources for the BMA include an Alleghanian Suture Zone (McBride & Nelson, 1988; Parker, 2014), rift-related mafic intrusions (Duff & Kellogg, 2019; Lizarralde et al., 1994), the negative anomaly component of a low-high pair with the ECMA from the breakup volcanic wedge (Austin et al., 1990) or a rift basin (the Brunswick Graben; Hutchinson et al., 1982).

The formation of the Atlantic Ocean followed continental breakup at the ENAM (Vogt, 1973). Various tectonic scenarios have been proposed for the early Atlantic opening. Scenarios such as a ridge jump (or two ridge jumps) (Bird et al., 2007; Klitgord & Schouten, 1986; Schettino & Turco, 2009; Vogt, 1973), asymmetric spreading that underwent a drastic change in rate and direction (Labails et al., 2010), or a period of protooceanic crust prior lithospheric rupture (Bécel et al., 2020; Shuck et al., 2019) between the ECMA and the Blake Spur Magnetic Anomaly (BSMA) (Figure 1) have been proposed to explain the wider domain of early ocean crust that is present offshore the ENAM compared to the conjugate margin offshore northwest Africa (Labails et al., 2010). Additionally, a spreading axis reorientation may have been present to accommodate the difference in strike between the initial seafloor spreading outboard of the ECMA and the modern Mid-Atlantic Ridge (Greene et al., 2017). Under all of the proposed scenarios, seafloor spreading rates for the early Atlantic indicate a slow-spreading regime (e.g., Bird et al., 2007; Greene et al., 2017; Klitgord & Schouten, 1986; Labails et al., 2010; Schettino & Turco, 2009), which continues in the present day (Müller et al., 2008).

The modern Mid-Atlantic Ridge displays along-strike segmentation at a similar spatial scale as the 100- to 150-km wavelength variation in ECMA amplitude (Figure 1b), suggesting that the segmentation of the Mid-Atlantic Ridge was inherited from rifting and breakup at the ENAM (Behn & Lin, 2000). While tracing fracture zones is challenging between the ECMA and anomaly M25 (Figure 1), the landward extrapolations of many Atlantic fracture zones align with offsets of linear magnetic anomalies identified between the ECMA and BSMA, suggesting that spreading center segmentation has persisted throughout the crustal evolution from continental breakup to the modern Mid-Atlantic Ridge (Greene et al., 2017; Klitgord & Schouten, 1986). Many of fracture zones in the Atlantic intersect the ENAM at magnetic lows that coincide with the 100- to 150-km wavelength ECMA amplitude variation (Figure 1) (Behn & Lin, 2000; Greene et al., 2017; Klitgord et al., 1988).

3. Methods

3.1. Data and Model Constraints

In this study, we use the North American Magnetic Anomaly Group (NAMAG) magnetic anomaly grid, composed of merged aeromagnetic and shipboard magnetic data, to model the volcanic wedge producing the ECMA (Figure 1) (Bankey et al., 2002). We merge available basement depth grids derived from U.S. Geological Survey (USGS) seismic reflection data in the Carolina Trough (Hutchinson et al., 1995) and Baltimore Canyon Trough/Georges Bank Basin (Klitgord et al., 1994) to create a margin-wide depth to basement grid that can be used to constrain the top of the volcanic wedge (Figure 2b). We also compiled available constraints on the extent of the volcanic wedge from previous interpretations of SDRs in deep-imaging seismic data at the ENAM, including the Federal Institute for Geosciences and Natural Resources (BGR) 1979

survey, Large Aperture Seismic Experiment (LASE), USGS Line 28, USGS Line 32, EDGE Line 801, BA-6, and the MGL1408 survey (Figure 2b) (Austin et al., 1990; Bécel et al., 2020; Hinz, 1981; Holbrook et al., 1994; Lase Study Group, 1986; Sheridan et al., 1993; Tréhu et al., 1989).

3.2. Magnetic Anomaly Modeling

We conducted 2-D and 3-D magnetic modeling of the volcanic wedge using the Fourier summation approach (Parker, 1973). We first created a series of 2-D magnetic forward models along profiles perpendicular to the ECMA (Figures S1 and S2 in the supporting information). Where available, we used SDR interpretations from previous studies to constrain the lateral extent of the volcanic wedge in these 2-D magnetic models (Figure 2b). The volcanic wedge geometry we use in our modeling increases in thickness from the inboard pinch-out toward a maximum thickness; then, it thins to zero in thickness as the volcanic wedge transitions into ocean crust on the outboard end (Figure S1). The modeled volcanic wedge geometries were interpolated between the 2-D magnetic model profiles along the margin to create an initial 3-D volcanic wedge for our 3-D magnetic modeling. The top of this 3-D modeled volcanic wedge was constrained using the seismically derived basement depth grid (Figure 2b). We then iteratively adjusted the lateral extent (perpendicular to the ECMA) and thickness (base) of the 3-D modeled volcanic wedge along the margin to achieve a calculated magnetic anomaly consistent with the observed ECMA amplitude and character (Figure 1a). We incorporate SDR interpretations made by previous studies of the ENAM (Figure 2b) to constrain the lateral extent of the volcanic wedge in our 3-D magnetic model. Both previous studies and our 2-D magnetic modeling suggest that the volcanic wedge extends landward and seaward of where SDRs are interpreted (Davis et al., 2018; Eldholm et al., 1995; Talwani et al., 1995) (Figure S1). Therefore, we use these SDRs interpretations (Figure 2b) as a minimum constraint on our modeled volcanic wedge extent, ensuring that our modeled volcanic wedge encompasses the full distribution of where SDRs have been identified at the margin. A maximum depth constraint for the base of our modeled volcanic wedge is the depth to the Curie temperature, as material below this depth would lose remanent magnetization and not contribute to the magnetic anomaly (Blakely, 1995; Rajaram, 2007). A global estimation based on magnetic anomaly inversion suggests that the Curie depth at the ENAM is greater than 27 km (Li et al., 2017) (Figure S4). We independently estimate the Curie depth to be ~23–25 km based on heat flow data collected at Site V20-232 (Pollack et al., 1993) (Figures 2a and S4).

Our 3-D magnetic model assumed a constant magnetization of 5 A/m throughout the volcanic wedge with an inclination of 45° and a declination of −2° based on the estimates of the Jurassic geomagnetic pole (Austin et al., 1990; Talwani et al., 1995). This magnetization is consistent with drilling results that penetrated SDRs at other margins (see Davis et al., 2018, their figure 3) and is similar to the magnetization used in 2-D magnetic modeling of volcanic wedges at both the ENAM (Figure S1) (Austin et al., 1990; Talwani et al., 1995) and other volcanic rifted margins (e.g., Bauer et al., 2000; Franke et al., 2019). We also validated this magnetization with a 2-D magnetization inversion (Figure S3) (Parker & Huestis, 1974). Davis et al. (2018) alternatively suggest that the ECMA is an induced, rather than remanent, magnetic anomaly produced by a 0.05 International System (SI) susceptibility volcanic wedge (present-day field inclination of 60°, declination of −10°, and strength of ~50,000 nT). A 5-A/m remanent volcanic wedge with Jurassic geomagnetic field directions produces a similar magnetic anomaly to a 0.05 SI-induced volcanic wedge with the steeper inclination of the present-day field (Behn & Lin, 2000; Davis et al., 2018). Therefore, we used a 5-A/m magnetization in our ECMA modeling, recognizing that an induced anomaly, or a combination of remanent and induced components, would result in a similar modeled volcanic wedge with comparable along-strike variations in thickness and width.

4. Results

4.1. Volcanic Wedge Distribution and Variations

Our magnetic modeling (Figure 3) shows that the volcanic wedge emplaced as the surficial component of the magmatism at the site of continental breakup can explain the ECMA (Figure 3) (Holbrook & Kelemen, 1993). Our modeled volcanic wedge mimics the strike of the ECMA and the modern-day shelf break along the margin. The top of the modeled volcanic wedge, derived from the seismically derived basement depth grid (Figure 2b), ranges from ~2–17 km in depth, with the greatest depths in the northern Baltimore Canyon Trough (Figure 3). The base of our modeled volcanic wedge, derived through our

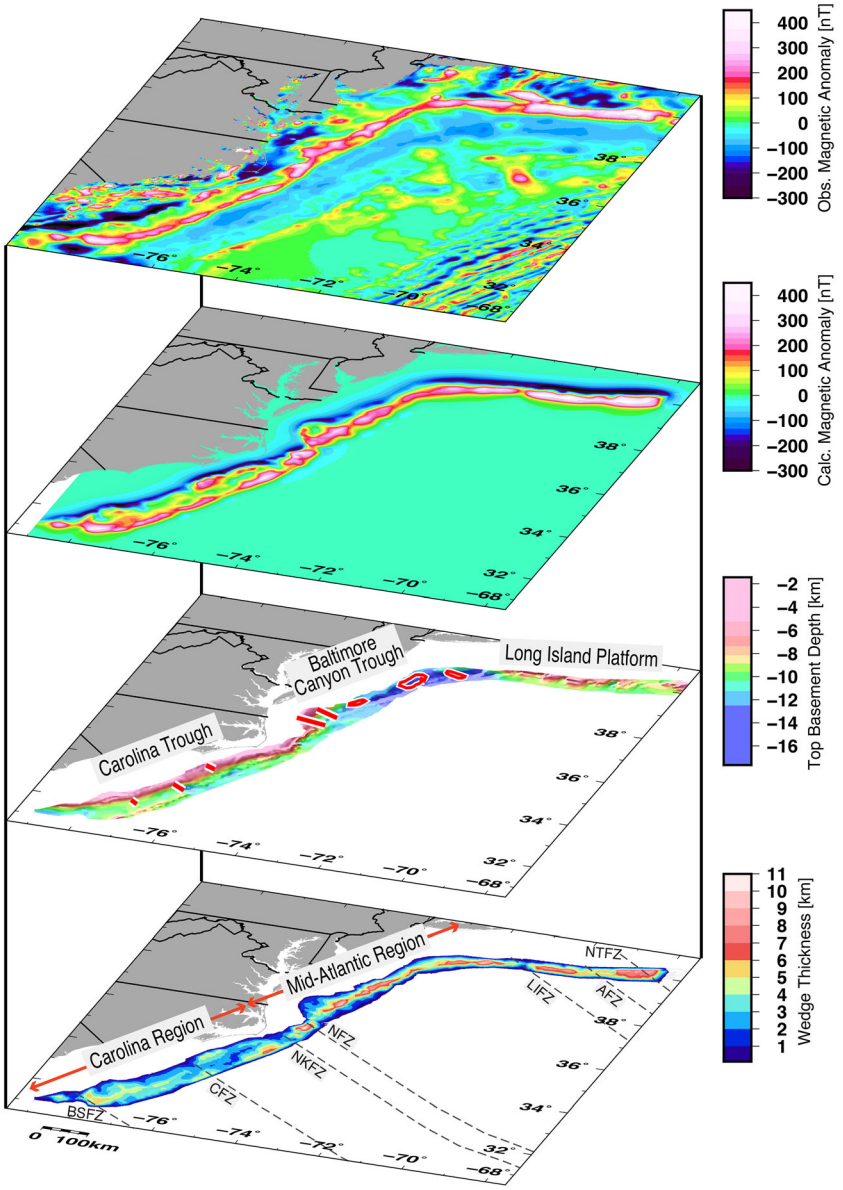

Figure 3. Results of 3-D magnetic forward modeling. From top to bottom: observed magnetic anomaly (Figure 1a), model calculated magnetic anomaly, top of modeled volcanic wedge from basement depth grid (Figure 2b), and modeled volcanic wedge thickness. Locations of SDR interpretations from previous studies indicated by red/white lines (Figure 2b). Gray dashed lines show landward extrapolations of major Atlantic fracture zones (Figure 1b) (Klitgord et al., 1988).

iterative 3-D forward modeling, ranges from ~14–23 km along the margin at its thickest points (Figure S5). The base of our modeled volcanic wedge is shallower than the Curie depths estimates for this area (~23–27 km; Figure S4), suggesting that the entire modeled volcanic wedge contributes to the magnetic anomaly signal.

The thickness and width of the volcanic wedge, derived from our iterative 3-D modeling, exhibits both first-order (~600–1,000 km) and second-order (~50–100 km) variations along the ENAM (Figures 3 and 4). The first-order volcanic wedge variation can be separated into two regions. The boundary separating the first-order variation in modeled volcanic wedge thickness and width is located near Cape Hatteras, North Carolina. South of this boundary (hereafter referred to as the Carolina Region), the modeled volcanic wedge has a more widely distributed thickness, corresponding to the broader, two-peak ECMA (Figure 3). The

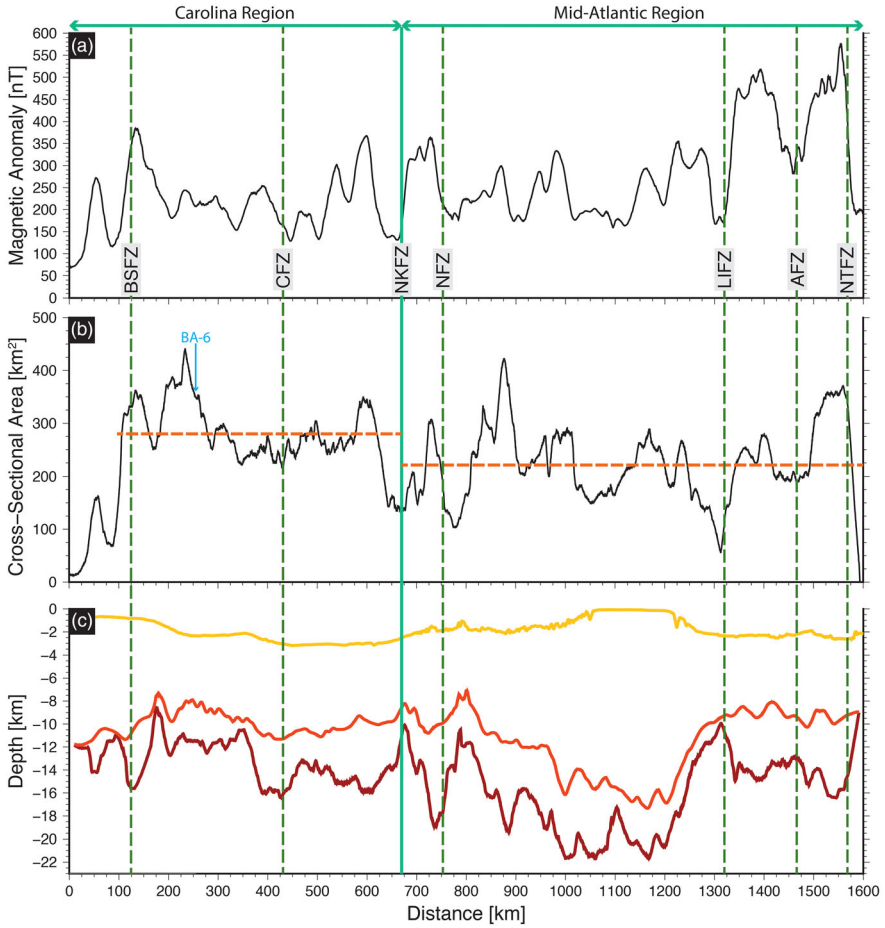

Figure 4. Along-margin profile along the ECMA axis (see Figure 1b). (a) Observed magnetic anomaly along-strike. (b) Modeled volcanic wedge cross-sectional area along strike. (c) Seafloor (orange), top of modeled volcanic wedge (from basement depth grid; Figure 2b) (red), and base of modeled volcanic wedge (dark red) beneath the ECMA axis. Extent of Carolina and Mid-Atlantic Regions marked. Red dashed lines show average cross-sectional areas for regions. Margin intersections of major Atlantic fracture zones indicated by green dashed lines (see Figure 1b) (Klitgord et al., 1988). Location of BA-6 (Austin et al., 1990) labeled.

maximum thicknesses of the modeled volcanic wedge in the Carolina Region are ~4–7 km. To the north of this boundary (hereafter referred to as the Mid-Atlantic Regions), the modeled volcanic wedge is thicker and has a more narrow distribution of thickness compared to the Carolina Region (Figure 3), corresponding with the higher-amplitude, single peak ECMA. The steeper thickening gradient reflects the overall narrower distribution of the modeled volcanic wedge thickness in the Mid-Atlantic Region. The maximum thickness of the modeled volcanic wedge in the Mid-Atlantic Region is ~7–10 km.

In the Carolina Region, the modeled volcanic wedge is able to replicate the positive, high-amplitude ECMA character and produces a thin, paired negative anomaly inboard of the ECMA (Figure 3). However, the strong negative amplitude and width of the BMA are not produced by the modeled volcanic wedge (Figure 3). This suggests that the BMA does not represent a low-high anomaly pair with the ECMA produced by the breakup volcanic wedge (e.g., Austin et al., 1990).

The overall modeled volcanic wedge thickness (Figure 3) is similar throughout the entire Mid-Atlantic Region. However, there is a difference in both the modeled volcanic wedge depth and orientation between the Baltimore Canyon Trough and Long Island Platform within the Mid-Atlantic Region, being present on either side of the prominent bend observed in the ECMA offshore the New York Bight (Figure 3). The strike of the volcanic wedge, and the ECMA, is north-south in the Baltimore Canyon Trough and more east-west on the Long Island Platform (Figure 3). The basement depth (representing the top of the modeled volcanic

wedge) is shallower on the Long Island Platform compared to the deep basement of the Baltimore Canyon Trough (Figures 2–4). A change in ECMA amplitude is coincident with these changes in basement depth and strike, being ~100–200 nT higher on the Long Island Platform compared to in the Baltimore Canyon Trough (Figures 1, 3, and 4). Both the strike and depth of the magnetic source body can influence magnetic anomaly amplitudes, which suggests that the higher ECMA amplitude on the Long Island Platform is not indicative of a greater amount of volcanic wedge emplacement; rather, it corresponds to a decrease in volcanic wedge (basement) depth and change in volcanic wedge strike within the Mid-Atlantic Region (e.g., Behn & Lin, 2000) (Figures 2–4).

The second-order variation in the thickness and width of our modeled volcanic wedge mimic the ~100- to 150-km wavelength amplitude variation along the ECMA (Behn & Lin, 2000) (Figures 3 and 4). Depth variation in the top of the basement has no apparent relationship with the 100- to 150-km wavelength ECMA amplitude variation, suggesting that this ECMA variation can be attributed to second-order segmentation of the volcanic wedge (Figures 3 and 4).

Magnetic anomalies can also be produced by variations in the distribution of magnetic source with different magnetization. In addition to the along-strike variations in the thickness and width of our modeled volcanic wedge at the ENAM, along-strike variations in the magnetization could conceivably arise from processes such as low temperature, long-term hydrothermal alteration (Pariso & Johnson, 1991) or partial cancelation of magnetization due to volcanic emplacement over alternating polarity periods (Davis et al., 2018). We test if along-strike variations in magnetization alone could explain the observed ECMA amplitude and character variation using a 3-D magnetic forward model with a constant volcanic wedge geometry. It was considerably challenging to reproduce both the amplitude and character of the ECMA simultaneously in the variable-magnetization model (Figure S6). It was particularly difficult to adjust the magnetization value alone to account for the ECMA amplitude without also causing a poor fit for the ECMA width, indicating that a spatial variation in the geometry of volcanics is likely needed to fully capture both the width and amplitude of the ECMA. We think this exercise supports the variable volcanic wedge thickness and width used in our 3-D magnetic modeling (Figure 3).

4.2. Volcanic Wedge Volume Estimates

Based on our interpretation of the magnetic forward modeling results, we estimate that the volcanic wedge emplaced as part of the ENAM breakup magmatism has a volume of ~373,000 km^3 from just south of the Blake Spur Fracture Zone to just north of the Nantucket Fracture Zone. Of this total volume, we estimate ~167,000 km^3 in the Carolina Region, with the remaining ~206,000 km^3 in the larger Mid-Atlantic Region.

We examined along-strike variations in the volume of the modeled volcanic wedge using changes in cross-sectional area (area perpendicular to the ECMA strike) as a proxy (Figure 4). The average cross-sectional area of the modeled volcanic wedge in the Carolina Region is ~280 km^2 (omitting the minor segment south of the Blake Spur Fracture Zone) and ranges between 220 and 450 km^2 between the centers and edges of the second-order geometry variations within this region (Figure 4). The average cross-sectional area of the modeled volcanic wedge in the Mid-Atlantic Region is ~225 km^2 and ranges between 75 and 450 km^2 between the centers and edges of the second-order geometry variations within this region (Figure 4). The average cross-sectional area of the Mid-Atlantic Region is comparatively smaller despite having a greater modeled volcanic wedge thickness, and this is due to the broader distribution of modeled volcanic wedge thickness in the Carolina Region (Figure 3).

Previous studies have estimated the volume of breakup volcanism at the ENAM (Austin et al., 1990; Talwani et al., 1995). Austin et al. (1990) estimate a cross-sectional area of 370 km^2 for the volcanic wedge on BA-6 (Figure 2), which consistent with the ~350 km^2 in our model (Figure 4). Extrapolating on this estimate, Austin et al. (1990) evaluate a total volcanic wedge volume of ~166,500 km^3 in the Carolina Trough, which is similar to the volume we estimate for our Carolina Region. Talwani et al. (1995) suggest a rough estimate of ~1×10^6 km^3 for the volcanic wedge by assuming that a 100-km-wide and 10-km-thick volcanic wedge extends 1,000 km along the margin. This estimate by Talwani et al. (1995) is larger than what we estimate due to their 10-km-thick volcanic wedge assumption, which is greater than what our modeling suggests is typical along the ENAM (Figure 3). Additionally, our modeling shows that a volcanic wedge with a constant along-strike geometry is not consistent with the observed variations in ECMA amplitude and character

(Figure 3). This discrepancy indicates that it is important to account for along-strike variations in volcanic wedge thickness and width when estimating the volume of breakup volcanism at rifted margins.

We can estimate the volume of mafic intrusives/underplating and the total (intrusive plus extrusive) volume of magmatism emplaced during continental breakup using the volume of volcanics based on our magnetic forward modeling results (Figure 3). Gallahue et al. (2020) found that the volumes of SDRs (volcanic wedge) are typically ~30% of the corresponding volume of high-velocity lower crust (mafic intrusives/underplating) interpreted on seismic reflection profiles at magma-rich rifted margins worldwide. Using this relationship, the volcanic wedge volume estimated from our magnetic forward modeling results (~373,000 km^3) suggests that ~1,243,000 km^3 of mafic intrusives/underplating was emplaced during breakup at the ENAM, yielding a total (intrusive plus extrusive) volume of ~1,616,000 km^3 for the focused breakup magmatism. This can be subdivided into mafic intrusives/underplating volumes of ~565,000 and ~687,000 km^3 in the Carolina and Mid-Atlantic Regions, respectively, and total breakup magmatism volumes of ~723,000 and ~893,000 km^3 in the Carolina and Mid-Atlantic Regions, respectively. Kelemen and Holbrook (1995) suggest that the total volume of breakup magmatism at the ENAM was as much as 2,700,000 km^3. This estimate by Kelemen and Holbrook (1995) is larger than what we estimate, as they only use two estimates for the geometry of SDRs and high-velocity lower crust (from Lines BA-6 and EDGE801; see Figure 2a) and extrapolate these dimensions along the entire margin, whereas we account for along-strike variations in the amount of magmatism.

5. Discussion

5.1. Margin-Scale Magmatism That Drove the Atlantic Opening

Magma-rich rifted continental margins, including the ENAM, bound 75% of the Atlantic Ocean and are the product of the breakup of Pangaea and the opening of the Atlantic Ocean (Eldholm et al., 2000; Menzies et al., 2002). The volcanic wedges emplaced at these margins serve as the surficial indicator of the margin-scale magmatism at the site of continental breakup (Holbrook & Kelemen, 1993; Keen & Potter, 1995). Understanding the amount of this margin-scale magmatism provides insight into a key component that can allow for continental breakup to occur at lower stress (Bialas et al., 2010; Buck, 2004; Daniels et al., 2014).

The dimensions of our modeled volcanic wedge are consistent with seismically determined SDRs, at the other magma-rich rifted continental margins of the Atlantic. At the North Atlantic Margins offshore Norway and Greenland, the volcanic wedge emplaced during breakup is ~20–100 km wide and ~4–6 km thick (Barton & White, 1997; Eldholm & Grue, 1994). At the southern South Atlantic Margin offshore Argentina and Uruguay, the volcanic wedge emplaced during breakup is 60–120 km in width and up to ~6–7 km thick (Franke et al., 2007, 2010). At the central South Atlantic conjugate margins offshore Brazil and Namibia, the volcanic wedge emplaced during breakup is ~50–200 km wide and up to 15 km thick (Koopmann et al., 2014; Talwani & Abreu, 2000). Our modeled volcanic wedge dimensions (~60–120 km wide and ~4–10 km thick) are similar to the dimensions observed at the other magma-rich Atlantic margins (Figure 3), which suggests that the margin-scale magmatism at the ENAM is typical of the amount of magmatism at magma-rich margins to drive the breakup of Pangaea and the Atlantic opening.

5.2. First-Order (~600–1,000 km) Magmatic Segmentation During Breakup at the ENAM

5.2.1. Rift Transfer Zone

Our modeling results show a first-order variation in the volcanic wedge width and thickness, separated into the Carolina and Mid-Atlantic Regions (Figure 3). The modeled volcanic wedge changes from a widely distributed thinner volcanic wedge in the Carolina Region to a narrower but thicker volcanic wedge in the Mid-Atlantic Region (Figure 3). This change indicates a first-order magmatic segmentation during breakup where each region experienced a different distribution and amount of magmatism (Figure 5), suggesting that key parameters controlling melt production likewise varied along the margin (e.g., Shuck et al., 2019; Withjack et al., 2012). One possible explanation for the change in character of the volcanic wedge is that a rift transfer zone exists just north of Cape Hatteras, which accommodated differences in extension between two rift segments experiencing different modes of magma emplacement during breakup (e.g., Bellahsen et al., 2013).

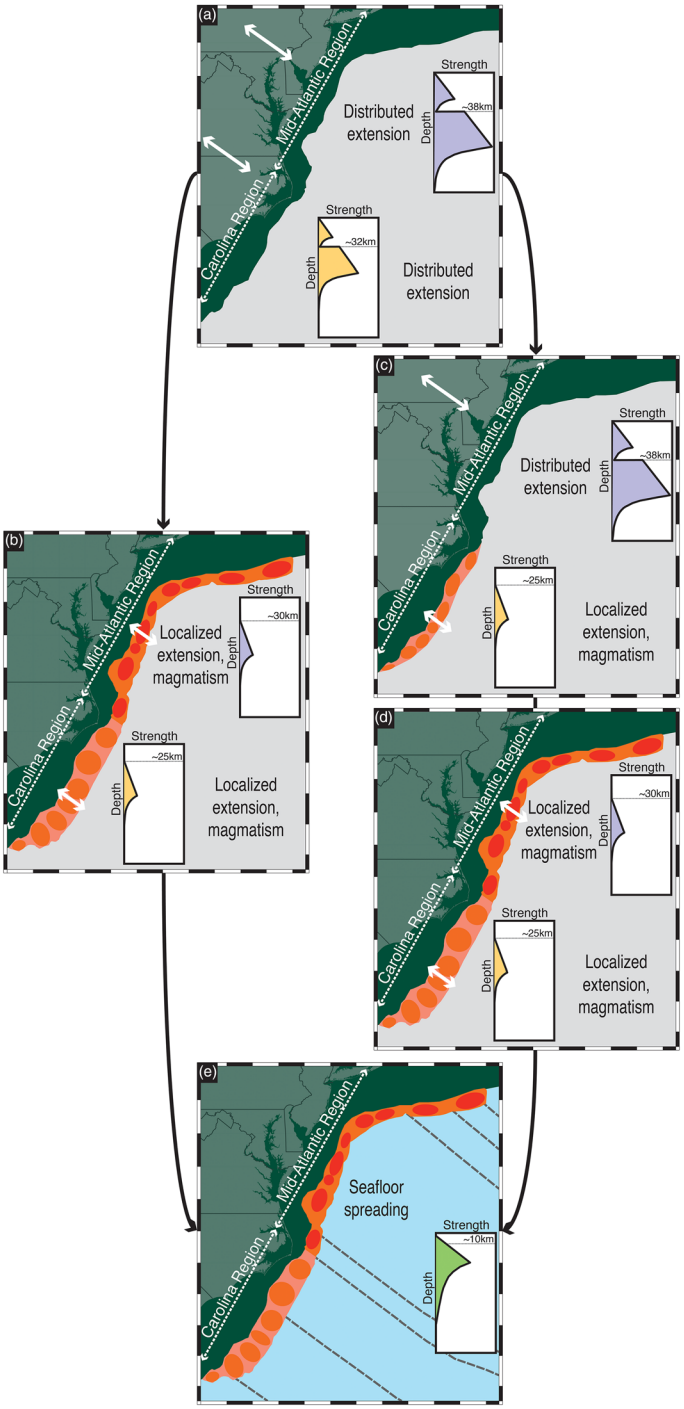

Figure 5. Schematic of rifting history with breakup magmatism at the ENAM. White arrows show approximate direction of extension. Volcanic wedge shown in orange; second-order segmentation shown with ovals; darker colors correspond to areas of a thicker volcanic wedge. Present-day coast and state boundaries shown for spatial reference. (a) Distributed extension onshore prior to breakup magmatism. (b) Volcanic wedge emplacement scenario with a synchronous localization of extension between the Carolina and Mid-Atlantic Regions. (c and d) Volcanic wedge emplacement scenario with an earlier localization of extension in the Carolina Region (panel c) and a later localization in the Mid-Atlantic Region (panel d). (e) Seafloor spreading following continental breakup; dashed lines indicate major Atlantic fracture zones (Figure 1a). Inset plots illustrate hypothetical lithosphere strength envelopes with possible effects of crustal thickness, rheological differences, and presence of magmatism on extension in the Carolina and Mid-Atlantic Regions (Buck, 2004, their figure 1.1; Lowrie, 2007, their figure 2.69; Marzen et al., 2019). Horizontal gray lines indicate crustal thickness (Marzen et al., 2019; Talwani et al., 1995).

Rift transfer zones are commonly observed in rifted continental margins (e.g., Bellahsen et al., 2013; Franke et al., 2007) and active rifts (e.g., Hayward & Ebinger, 1996; Manighetti et al., 2001) to divide a rift into distinct regions. Transfer zones accommodate differences in extension between rift segments through a system of faults that can be oriented subperpendicular or subparallel to the rift (Bellahsen et al., 2013; Hayward & Ebinger, 1996; Manighetti et al., 2001). While it is typically not feasible to directly map this system of faults buried under thick sediment at rifted continental margins, like can be done in active rift settings (e.g., Hayward & Ebinger, 1996; Manighetti et al., 2001), key diagnostic features can be observed that indicate the presence of a transfer zone at rifted continental margins, including a step over (e.g. lateral offset) in the volcanic wedge and a change in volcanic wedge volume and distribution on either side of the transfer zone (Franke et al., 2007).

The change in the modeled volcanic wedge width and thickness near Cape Hatteras, and the lateral offset in both the ECMA and the modeled volcanic wedge, suggests that a rift transfer zone was present between the Carolina and Mid-Atlantic Regions during continental breakup, hereafter referred to as the Hatteras Transfer Zone (Figure 3). Transfer zones have been observed in some cases to form at preexisting zones of weakness, such as at suture zones between accreted geologic terranes (Bellahsen et al., 2013; Franke et al., 2007). The Hatteras Transfer Zone coincides with possible preexisting weaknesses produced by tectonic amalgamation during the construction of Pangaea (Boote & Knapp, 2016; Hatcher, 2002; Lefort & Max, 1991). The Hatteras Transfer Zone is located just north of the Alleghanian suture zone separating the pre-Alleghanian Laurentian terranes to the northwest from the (peri-)Gondwanan accreted terranes to the southeast (Figure 2b) (Boote & Knapp, 2016; Hatcher, 2002). It also aligns with an inferred suture zone between Laurentian terranes and a piece of the Archean West African Craton that has been hypothesized to underlie the Chesapeake Bay (Figure 2b) (Lefort & Max, 1991); however, others have alternatively suggested Laurentian crust beneath Chesapeake Bay, precluding the presence of this suture zone (Sheridan et al., 1999). The Alleghanian suture zone, and/or the possible West African Craton suture, represents preexisting weakness that is spatially correlated with, and could have led to the formation of, the Hatteras Transfer Zone (Figure 2b). The presence of the BMA in the Carolina Region and absence in the Mid-Atlantic Region (Klitgord et al., 1988) provide additional support for the Hatteras Transfer Zone. Suggested magnetic sources for the BMA imply tectonic and magmatic rift activity (e.g., extension on a suture zone, rift basin formation, or rift-related mafic intrusions) in the Carolina Region that does not extend northward into the Mid-Atlantic Region (e.g., Duff & Kellogg, 2019; Hutchinson et al., 1982; Lizarralde et al., 1994; McBride & Nelson, 1988; Parker, 2014), and the boundary of this activity could be the Hatteras Transfer Zone.

The coincidence of the Hatteras Transfer Zone, separating the first-order change in the modeled volcanic wedge geometry, with an inferred suture zone (Boote & Knapp, 2016; Hatcher, 2010; Lefort & Max, 1991) shows the possible influence of zones of weakness between amalgamated geologic terranes on the subsequent period of rifting and continental breakup. The Hatteras Transfer Zone also represents a key structural element of the rift that separates the first-order magmatic segmentation characterized by two regions with distinct modes of magma emplacement during breakup. The distinct modes of magma emplacement in these two regions were likely governed by parameters present during continental breakup, including the mantle temperature and the mode of crustal extension/thinning, can control the amount and distribution of magmatism (Figure 5) (e.g., Keir et al., 2013; Koopmann et al., 2014; White et al., 2008; White & McKenzie, 1989).

5.2.2. Along-Margin Increase in Mantle Temperature

Mantle temperature plays a key role in magma production in rifts (Shuck et al., 2019; White et al., 2008; White & McKenzie, 1989). Understanding along-margin changes in mantle temperature and the associated magma production identify where greater extension accommodation and thermal weakening was present to enable continental breakup at lower stress (Bialas et al., 2010; Buck, 2004).

Margin-wide variations in the thickness of our modeled volcanic wedge (Figure 3) suggest that a south to north increase in mantle temperature could have been present during breakup at the ENAM across the Hatteras transfer zone, as warmer mantle temperatures can enhance melting to create greater magma production and a thicker volcanic package (White et al., 1987). The comparatively thicker modeled volcanic wedge emplaced over a narrower zone in the Mid-Atlantic Region could be caused by a higher amount of melt production related to a warmer mantle temperature beneath this region (Figures 3, 5b, and 5d). The comparatively wider but thinner modeled volcanic wedge in the Carolina Region could be caused by a lower amount of melt production related to a cooler mantle temperature beneath this region (Figures 3 and 5b–5d).

Shuck et al. (2019) use seismic velocities and petrological modeling of the MGL1408 seismic data to infer an ~2-km increase in the margin crustal thickness and ~10–25°C increase in mantle temperature from south to north across the zone we call the Hatteras Transfer Zone (Figure 2a). The south to north increase in our modeled volcanic wedge thickness between the Carolina and Mid-Atlantic Regions is consistent with this mantle temperature and crustal thickness trend (Figure 3) (Shuck et al., 2019).

A difference in the prebreakup continental crustal thickness, related to a difference in basement terranes acquired during the amalgamation of Pangaea, could have been present prior to breakup at the ENAM. This difference could impact the amount of thermal insulation and the mantle temperature during breakup (Shuck et al., 2019). The Hatteras Transfer Zone is located just north of the Alleghanian suture zone (Boote & Knapp, 2016; Hatcher, 2002) (Figure 2b). This suture zone separates the thicker crust (~38 km) of the pre-Alleghanian Laurentian terranes, inboard of the Mid-Atlantic Region, from the thinner crust (~32 km) of the (peri-)Gondwanan terranes in the Carolina Region (Marzen et al., 2019). The thicker pre-Alleghanian Laurentian crust could provide more thermal insulation that would cause a comparatively higher mantle temperature in the Mid-Atlantic Region compared to the Carolina Region (Shuck et al., 2019). This difference in the thickness of the preexisting continental crust between the Carolina and Mid-Atlantic Regions could cause a south to north increase in mantle temperature (Marzen et al., 2019; Shuck et al., 2019), which we suggest is responsible for the south to north increase in melt production and the related increase in the thickness of our modeled volcanic wedge (Figure 3).

Along-margin changes in mantle temperature can also be related to the presence of a mantle plume (Ebinger & Sleep, 1998). It has been proposed that mantle plumes can induce continental breakup (Courtillot et al., 1999). Mantle temperatures, and therefore the scale of magmatism, decreases radially from the location of a mantle plume (Ebinger & Sleep, 1998; Holbrook & Kelemen, 1993). However, the relatively abrupt change, rather than systematic decrease, in our modeled volcanic wedge thickness suggest a similar abrupt change in mantle temperature that is not consistent with a mantle plume (Figures 3 and 4). Furthermore, while a mantle plume has been proposed to explain the CAMP volcanism and the (either coeval or later) breakup magmatism at the ENAM (Courtillot et al., 1999; White & McKenzie, 1989; Wilson, 1997), the existence of this plume has been debated (Marzoli et al., 2018). Available evidence, including magma geochemistry data, the timing and extent magmatism, the absence of a crustal thickness anomaly, and a lack of a Jurassic hotspot track, does not currently support the presence of a mantle plume (Holbrook & Kelemen, 1993; Kelemen & Holbrook, 1995; Marzoli et al., 2018; McHone, 2000).

5.2.3. Degree of Crustal Extension and Thinning

Variations in the timing and amount of extension localization and crustal thinning can influence the duration, location, and amount of magma production during continental breakup (e.g., Armitage et al., 2010; Franke et al., 2007; Keir et al., 2013; Koopmann et al., 2014). The first-order variations in the width and thickness of our modeled volcanic wedge (Figure 3) are consistent with a variation in the timing and amount of extension localization and crustal thinning at the ENAM, and the associated amount and duration breakup magmatism, between the Carolina and Mid-Atlantic Regions (e.g., Withjack et al., 2012), with the Hatteras Transfer Zone accommodating the differences in extension between these two regions.

After a period of broadly distributed extension during the Late Triassic rifting at the ENAM (Figure 5a), crustal extension and thinning became localized near the site of eventual continental breakup and was accommodated by magmatism and volcanic wedge emplacement (Withjack et al., 1998). If the timing of extension localization was synchronous along the southern ENAM, both the Mid-Atlantic and Carolina Regions would have experienced a similar duration of breakup magmatism, and the first-order variations in the geometry of our modeled volcanic wedge would be the result of a different spatial distribution of magmatic emplacement (Figure 3). In this scenario, the wider modeled volcanic wedge in the Carolina Region would be the result of a wider zone of magmatic emplacement compared to the narrower volcanic wedge in the Mid-Atlantic Region (Figure 5b). However, the first-order variation in the geometry of our modeled volcanic wedge (Figure 3) could instead be explained by a temporal difference in magmatic emplacement (Figures 5c and 5d). Onshore rift basin activity and inferred timings of volcanic wedge emplacement suggest that the localization of crustal extension and initiation of volcanic wedge emplacement along the southern ENAM may have been diachronous, occurring earlier in the Carolina Trough and later in the Baltimore Canyon Trough (Schlische et al., 2003; Withjack et al., 2012). The wider zone of volcanic wedge emplacement in the Carolina Region suggested by our model is consistent with a prolonged period of breakup magmatism

(Figures 3 and 5c), which would result from an earlier localization of extension (Withjack et al., 2012). This longer period of breakup magmatism would have also released heat, which could help additionally explain the inferred lower mantle temperature in the Carolina Region (Shuck et al., 2019). The narrower zone of modeled volcanic wedge emplacement in the Mid-Atlantic Region could be caused by a comparatively later localization of extension and a briefer duration of breakup magmatism, with the narrower lateral extent causing vertical piling of the volcanic layers and the thicker modeled volcanic wedge in this region (Figures 3 and 5d). While this magmatic emplacement occurred in the Mid-Atlantic Region, magmatic emplacement would have continued to the south in the Carolina Region (Figure 5d). Following volcanic wedge emplacement in both regions, seafloor spreading began producing oceanic (or protooceanic) crust outboard of the ECMA (Figure 5e) (Klitgord & Schouten, 1986; Labails et al., 2010; Schettino & Turco, 2009; Shuck et al., 2019).

Withjack et al. (2012) suggest that the boundary between the diachronous localization of extension and volcanic wedge emplacement is located near Chesapeake Bay, occurring earlier to the south and later to the north. If the variations in the distribution and amount of breakup magmatism between the Carolina and Mid-Atlantic Regions are the result of a temporal difference in extension localization, we suggest that this boundary should instead be located slightly to the south, near Cape Hatteras (Figure 3). This location coincides with Hatteras Transfer Zone and is just north of an Alleghanian suture zone (Figure 2b) between the pre-Alleghanian Laurentian terranes (to the northwest), and the (peri-)Gondwanan accreted terranes (to the southeast) (Boote & Knapp, 2016; Hatcher, 2010; Higgins & Zietz, 1983). Marzen et al. (2019) suggest that the rheology of the thinner Gondwanan terranes, which make up much of the Carolina Region, may have made the crust in this region easier to extend during the rifting of Pangaea compared to the thicker pre-Alleghanian Laurentian terranes that predominantly make up the Mid-Atlantic Region. The combination a regional difference in geologic terranes and crustal thickness could have influenced the timing of extension localization and the associated duration of breakup magmatism (e.g., Withjack et al., 2012), occurring first in the Carolina Region and later in the Mid-Atlantic Region (Figures 5c and 5d).

5.3. Second-Order (~50–100 km) Magmatic Segmentation During Breakup at the ENAM

The signature of the current Wilson cycle is present within second-order magmatic segmentation that developed during breakup at the ENAM. Amplitude variation (100- to 150-km wavelength) observed in the ECMA and margin isostatic gravity anomaly suggests that the ENAM is segmented along the margin (Figure 1a) (Behn & Lin, 2000). Magmatic segmentation at a similar scale is a feature in modern active rifts, such as the East African Rift and Afar, and indicates along-strike variations in the amount of magmatism and tectonic strain available to accommodate the transition to mid-ocean ridge seafloor spreading (e.g., Beutel et al., 2010; Ebinger & Casey, 2001; Keir et al., 2013; Kendall et al., 2005; Manighetti et al., 1998, 2001). The along-margin variations in the width and thickness of our modeled volcanic wedge, which mimic the 100- to 150-km-wavelength amplitude variation in the ECMA, suggest that analogous, second-order magmatic segmentation was present during breakup at the ENAM (Figures 3–5). This second-order magmatic segmentation exists within the first-order magmatic segmentation (Figures 3–5), which has similarly been observed in Afar (Manighetti et al., 2001), suggesting an independent cause for this segmentation. Following continental breakup, the segmentation of the ensuing Mid-Atlantic Ridge may have been inherited from the magmatic segmentation at the ENAM (Behn & Lin, 2000).

The cause of second-order magmatic segmentation in both active rifts and mid-ocean ridges is thought to be along-strike variations in melt production, tectonic strain, and/or melt transport (e.g., Geoffroy, 2001; Magde & Sparks, 1997; Manighetti et al., 1998; Whitehead et al., 1984). Variations in melt production can increase the amount of magma at the center of each segment and have been attributed to focused upwelling of warmer asthenospheric mantle associated with small-scale convection beneath the center of the discrete segments (Geoffroy, 2001; Lin et al., 1990). Magmatic segmentation can also be the product of tectonic strain (Manighetti et al., 2001), with decompression melting and dike intrusions at the segment centers (Ebinger & Casey, 2001). Alternatively, melt transport at the base of the lithosphere can focus magma into the center of each segment (e.g., Magde & Sparks, 1997). Melt produced over a wide area rises vertically to the base of the lithosphere and can be transported along this boundary (Keir et al., 2015; Magde & Sparks, 1997). This transport process is facilitated by buoyancy driven flow and topography at the base of the lithosphere (Ebinger & Sleep, 1998). Topography at the base of the lithosphere can be induced by variations in the

amount of extension and thinning, which creates locally shallower points beneath the segment centers to facilitate melt focusing (Shillington et al., 2009).

The second-order magmatic segmentation at the ENAM during breakup could be explained by focused upwelling in the asthenosphere, tectonic strain, and/or magma transport at the base of the lithosphere. While it is difficult to identify which of these processes were present at the ENAM during breakup based solely on magnetic modeling of the volcanic wedge, these processes have been inferred to cause analogous segmentation at other rifts worldwide and could have plausibly been present at the ENAM. Focused upwelling has been proposed as a mechanism causing modern magmatic segmentation in the Afar depression of the East African Rift (Gallacher et al., 2016; Hammond et al., 2013), the Gulf of California (Wang et al., 2009), and mid-ocean ridges (Lin et al., 1990; Schouten et al., 1985; Sempéré et al., 1993; Whitehead et al., 1984). Magmatic segmentation documented in Afar has also been attributed to tectonic strain (Manighetti et al., 2001). Melt transport at the base of the lithosphere has been proposed to cause magmatic segmentation in the East African Rift (Keir et al., 2015), the eastern Black Sea (Shillington et al., 2009), and mid-ocean ridges (Magde & Sparks, 1997).

The consistency in the along-strike length scale of the second-order segmentation is intrinsically related to the underlying mechanism at the rift (e.g., Lin et al., 1990; Magde & Sparks, 1997), and the fairly regular 100- to 150-km spacing of the second-order segmentation in our magnetic modeling (Figures 3 and 4) provides insight into the scale and regularity of the causative mechanism along the ENAM. If the second-order magmatic segmentation at the ENAM was caused by focused asthenospheric upwelling, the second-order volcanic wedge segments in our modeling (Figure 3) indicate the location and periodicity of small-scale convection cells that developed in the underlying asthenosphere during breakup (e.g., Geoffroy, 2001). Alternatively, if the second-order magmatic segmentation was produced by tectonic strain, the second-order volcanic wedge segments (Figure 3) indicate the distribution of tectonic strain and dike intrusion during breakup (e.g., Ebinger & Casey, 2001). Finally, if the second-order magmatic segmentation was caused by melt transport at the base of the lithosphere, the second-order volcanic wedge segments identify where the melt was focused (Figure 3) and may indicate locations that experienced greater extension and thinning during rifting (e.g., Shillington et al., 2009).

The length scales of the segmentation in mid-ocean ridges and the magmatic segmentation observed in rifts are equivalent, which indicates that the segmentation of the spreading centers may be inherited from the rifting and breakup process (e.g., Behn & Lin, 2000; Beutel et al., 2010; Hayward & Ebinger, 1996). Mid-ocean ridge transform faults can originate from both rift transfer zones, related to preexisting zones of weakness at the suture zones between geologic terranes accreted during previous Wilson cycles, and from the magmatic segmentation present during breakup (Bellahsen et al., 2013; Franke et al., 2007). At the ENAM, both the Hatteras Transfer Zone, separating the first-order magmatic segmentation, and the second-order magmatic segmentation present during breakup likely influenced the segmentation and transform fault formation in the ensuing Mid-Atlantic Ridge.

At the ENAM, the Hatteras Transfer Zone may have facilitated the inheritance of a Mid-Atlantic Ridge transform fault from preexisting structure (i.e., zones of weakness associated with suture zones), as has been hypothesized for rifted continental margins worldwide (e.g., Bellahsen et al., 2013; Franke et al., 2007). The landward extrapolation of the Northern Kane Fracture Zone (Klitgord & Schouten, 1986) and offsets in the linear magnetic anomalies between the ECMA and BSMA (Greene et al., 2017) intersect the ENAM just north of Cape Hatteras, coincident with the Hatteras Transfer Zone (Figures 1b and 3) and near inferred suture zones between geologic terranes associated with the Alleghanian continental collision (Figure 2b) (Boote & Knapp, 2016; Hatcher, 2002; Lefort & Max, 1991). The spatial relation of these features suggests that the Mid-Atlantic Ridge transform fault offset producing the Northern Kane Fracture Zone may have been inherited from preexisting structure associated with the continental collisions that built Pangaea, and this inheritance was facilitated by the Hatteras Transfer Zone during breakup.

Numerous transform faults of the early and modern Mid-Atlantic Ridge may have formed from the second-order magmatic segmentation during breakup at the ENAM (Figure 3). The second-order magmatic segmentation suggested by our modeling, and the ECMA amplitude variation, exists on a similar length scale to the Mid-Atlantic Ridge segmentation (Behn & Lin, 2000). The landward extrapolation of many Atlantic fracture zones (Klitgord & Schouten, 1986) aligns with offsets in the linear magnetic anomalies

between the ECMA and BSMA (Greene et al., 2017), suggesting that these fracture zones persist back to the margin. These fracture zones also intersect the margin between, or close to, our modeled volcanic wedge segments and the Hatteras Transfer Zone (Figures 1b, 3, and 4). The combination of similar segmentation scales and coincident fracture zone locations suggests that the ensuing spreading center segmentation, which persists in the modern Mid-Atlantic Ridge, was inherited from the magmatic segmentation during breakup at the ENAM (Figure 5e) (e.g., Behn & Lin, 2000). This genetic relationship between breakup and seafloor spreading at the ENAM supports the hypothesis that mid-ocean ridge segmentation develops from the magmatic segmentation and transfer zones associated with continental breakup, linking the rifting and seafloor spreading stages of the Wilson cycle (e.g., Bellahsen et al., 2013; Beutel et al., 2010; Collier et al., 2017; Hammond et al., 2013; Hayward & Ebinger, 1996; Keranen et al., 2004).

6. Conclusions

The results of our three-dimensional magnetic modeling suggest that the ECMA is produced by a combination of first-order (~600–1,000 km) and second-order (~50–100 km) magmatic segmentation, indicating along-margin variations in the distribution and amount of the magmatism that drove continental breakup at the ENAM. The two regions representing the first-order magmatic segmentation were likely separated by a rift transfer zone (here called the Hatteras Transfer Zone) and could be related to differences in mantle temperature and/or the timing and amount of crustal extension/thinning, both of which are probably governed by preexisting variations in crustal thickness and rheology developed during the tectonic amalgamation of Pangaea. The second-order magmatic segmentation likely represents along-margin variations in magma production and/or transport during breakup at the ENAM. Using a margin-wide investigation approach, we augmented the previously proposed model that the magmatic segmentation during breakup likely influenced the segmentation and transform fault spacing of the initial, and modern, Mid-Atlantic Ridge. Our study highlights the strength of magnetic anomaly data, which has a more extensive and continuous coverage than other data types, as a prime tool to comprehensively investigate the margin-wide, three-dimensional distribution and amount of magmatism at rifted continental margins.

Data Availability Statement

Data used in this study are available from U.S. Geological Survey Open-File Reports 94-637 (Klitgord et al., 1994), 97-27 (Hutchinson et al., 1995), and 02-414 (Bankey et al., 2002). See supporting information for additional magnetic modeling results used in this study.

Acknowledgments

Thanks to Anne Bécel, Dan Lizarralde, Collin Brandl, Brandon Shuck, and Mark Everett for beneficial discussion and assistance in compiling the archived data used in this study. We thank Debbie Hutchinson (USGS Woods Hole Coastal and Marine Science Center) for passing along her vast breadth of knowledge on the ENAM through numerous constructive suggestions to greatly strengthen our manuscript. We greatly appreciate the insightful comments from two reviewers, the Associate Editor, and the Editor that significantly improved the manuscript. Thanks to Maurice Tivey for providing codes that aided our magnetic modeling efforts. Project completed as part of J.A.G.'s Ph.D. dissertation at Texas A&M University.

References

Ajay, K., Chaubey, A., Krishna, K., Rao, D. G., & Sar, D. (2010). Seaward dipping reflectors along the SW continental margin of India: Evidence for volcanic passive margin. *Journal of Earth System Science*, *119*(6), 803–813. https://doi.org/10.1007/s12040-010-0061-2

Almalki, K. A., Betts, P. G., & Ailleres, L. (2015). The Red Sea—50 years of geological and geophysical research. *Earth-Science Reviews*, *147*, 109–140. https://doi.org/10.1016/j.earscirev.2015.05.002

Alsop, L. E., & Talwani, M. (1984). The East Coast Magnetic Anomaly. *Science*, *226*(4679), 1189–1191. https://doi.org/10.1126/science.226.4679.1189

Amante, C., & Eakins, B. W. (2009). *ETOPO1 1 arc-minute global relief model: Procedures, data sources and analysis, NOAA technical memorandum NESDIS NGDC-24*. Boulder, CO: National Geophysical Data Center, Marine Geology and Geophysics Division.

Armitage, J. J., Collier, J. S., & Minshull, T. A. (2010). The importance of rift history for volcanic margin formation. *Nature*, *465*(7300), 913–917. https://doi.org/10.1038/nature09063

Austin, J. A. Jr., Stoffa, P. L., Phillips, J. D., Oh, J., Sawyer, D. S., Purdy, G. M., et al. (1990). Crustal structure of the Southeast Georgia embayment-Carolina trough: Preliminary results of a composite seismic image of a continental suture (?) and a volcanic passive margin. *Geology*, *18*(10), 1023–1027. https://doi.org/10.1130/0091-7613(1990)018<1023:CSOTSG>2.3.CO;2

Autin, J., Leroy, S., Beslier, M. O., d'Acremont, E., Razin, P., Ribodetti, A., et al. (2010). Continental break-up history of a magma-poor margin based on seismic reflection data (northeastern Gulf of Aden margin, offshore Oman). *Geophysical Journal International*, *180*(2), 501–519. https://doi.org/10.1111/j.1365-246X.2009.04424.x

Bankey, V., Cuevas, A., Daniels, D., Finn, C.A., Hernandez, I., Hill, P., et al. (2002). Digital data grids for the magnetic anomaly map of North America. *U.S. Geological Survey Open-File Report 02–414*.

Barton, A., & White, R. (1997). Volcanism on the Rockall continental margin. *Journal of the Geological Society*, *154*(3), 531–536. https://doi.org/10.1144/gsjgs.154.3.0531

Bastow, I. D., & Keir, D. (2011). The protracted development of the continent-ocean transition in Afar. *Nature Geoscience*, *4*(4), 248–250. https://doi.org/10.1038/ngeo1095

Bauer, K., Neben, S., Schreckenberger, B., Emmermann, R., Hinz, K., Fechner, N., et al. (2000). Deep structure of the Namibia continental margin as derived from integrated geophysical studies. *Journal of Geophysical Research*, *105*(B11), 25,829–25,853. https://doi.org/10.1029/2000JB900227

Bécel, A., Davis, J. K., Shuck, B. D., Van Avendonk, H. J. A., & Gibson, J. C. (2020). Evidence for a Prolonged Continental Breakup Resulting From Slow Extension Rates at the Eastern North American Volcanic Rifted Margin. *Journal of Geophysical Research: Solid Earth*, *125*, e2020JB020093. https://doi.org/10.1029/2020JB020093

Behn, M. D., & Lin, J. (2000). Segmentation in gravity and magnetic anomalies along the US East Coast passive margin: Implications for incipient structure of the oceanic lithosphere. *Journal of Geophysical Research*, *105*(B11), 25,769–25,790. https://doi.org/10.1029/2000JB900292

Bellahsen, N., Leroy, S., Autin, J., Razin, P., d'Acremont, E., Sloan, H., et al. (2013). Pre-existing oblique transfer zones and transfer/transform relationships in continental margins: New insights from the southeastern Gulf of Aden, Socotra Island, Yemen. *Tectonophysics*, *607*, 32–50. https://doi.org/10.1016/j.tecto.2013.07.036

Berndt, C., Planke, S., Alvestad, E., Tsikalas, F., & Rasmussen, T. (2001). Seismic volcanostratigraphy of the Norwegian Margin: Constraints on tectonomagmatic break-up processes. *Journal of the Geological Society*, *158*(3), 413–426.

Beutel, E., van Wijk, J., Ebinger, C., Keir, D., & Agostini, A. (2010). Formation and stability of magmatic segments in the Main Ethiopian and Afar rifts. *Earth and Planetary Science Letters*, *293*(3–4), 225–235. https://doi.org/10.1016/j.epsl.2010.02.006

Bialas, R. W., Buck, W. R., & Qin, R. (2010). How much magma is required to rift a continent? *Earth and Planetary Science Letters*, *292*(1–2), 68–78. https://doi.org/10.1016/j.epsl.2010.01.021

Biari, Y., Klingelhoefer, F., Sahabi, M., Funck, T., Benabdellouahed, M., Schnabel, M., et al. (2017). Opening of the central Atlantic Ocean: Implications for geometric rifting and asymmetric initial seafloor spreading after continental breakup. *Tectonics*, *36*, 1129–1150. https://doi.org/10.1002/2017TC004596

Bird, D., Hall, S., Burke, K., Casey, J., & Sawyer, D. (2007). Early central Atlantic Ocean seafloor spreading history. *Geosphere*, *3*(5), 282–298. https://doi.org/10.1130/GES00047.1

Blackburn, T. J., Olsen, P. E., Bowring, S. A., McLean, N. M., Kent, D. V., Puffer, J., et al. (2013). Zircon U-Pb geochronology links the end-Triassic extinction with the Central Atlantic Magmatic Province. *Science*, *340*(6135), 941–945. https://doi.org/10.1126/science.1234204

Blakely, R. J. (1995). *Potential theory in gravity and magnetic applications*. Cambridge, UK: Cambridge university press.

Boillot, G., Grimaud, S., Mauffret, A., Mougenot, D., Kornprobst, J., Mergoil-Daniel, J., & Torrent, G. (1980). Ocean-continent boundary off the Iberian Margin: A serpentinite diapir west of the Galicia Bank. *Earth and Planetary Science Letters*, *48*, 23–34.

Boote, S. K., & Knapp, J. H. (2016). Offshore extent of Gondwanan Paleozoic strata in the southeastern United States: The Suwannee suture zone revisited. *Gondwana Research*, *40*, 199–210. https://doi.org/10.1016/j.gr.2016.08.011

Bradley, D. C. (2008). Passive margins through earth history. *Earth-Science Reviews*, *91*(1–4), 1–26.

Brune, S. (2016). Rifts and rifted margins: A review of geodynamic processes and natural hazards. In J. C. Duarte & W. P. Schellart (Eds.), *Plate boundaries and natural hazards*, *AGU Geophysical Monograph 219*. American Geophysical Union. https://doi.org/10.1002/9781119054146.ch2

Buck, W. R. (2004). Consequences of asthenospheric variability on continental rifting. In G. D. Karner, B. Taylor, N. W. Driscoll, D. L. Kohlstedt (Eds.), *Rheology and deformation of the lithosphere at continental margins* (pp. 1–31). Columbia: Columbia University Press.

Buck, W. R. (2006). The role of magma in the development of the Afro-Arabian Rift System. In G. Yirgu, C. J. Ebinger, P. K. H. Maguire (Eds.), *The Afar volcanic province within the East African Rift System*, *Special Publications* (Vol. 259, pp. 43–54). London: Geological Society.

Buck, W. R. (2017). The role of magmatic loads and rift jumps in generating seaward dipping reflectors on volcanic rifted margins. *Earth and Planetary Science Letters*, *466*, 62–69. https://doi.org/10.1016/j.epsl.2017.02.041

Chaytor, J. D., Uri, S., Solow, A. R., & Andrews, B. D. (2009). Size distribution of submarine landslides along the US Atlantic margin. *Marine Geology*, *264*(1–2), 16–27.

Collier, J. S., McDermott, C., Warner, G., Gyori, N., Schnabel, M., McDermott, K., & Horn, B. W. (2017). New constraints on the age and style of continental breakup in the South Atlantic from magnetic anomaly data. *Earth and Planetary Science Letters*, *477*, 27–40. https://doi.org/10.1016/j.epsl.2017.08.007

Corner, B., Cartwright, J., & Swart, R. (2002). Volcanic passive margin of Namibia: A potential fields perspective. In M. A. Menzies, S. L. Klemperer, C. J. Ebinger, J. Baker (Eds.), *Volcanic rifted margins* (pp. 203–220). Boulder, CO: Geological Society of America Special Paper 362.

Courtillot, V., Jaupart, C., Manighetti, I., Tapponnier, P., & Besse, J. (1999). On causal links between flood basalts and continental breakup. *Earth and Planetary Science Letters*, *166*, 177–195.

d'Acremont, E., Leroy, S., Beslier, M.-O., Bellahsen, N., Fournier, M., Robin, C., et al. (2005). Structure and evolution of the eastern Gulf of Aden conjugate margins from seismic reflection data. *Geophysical Journal International*, *160*, 869–890.

Daniels, K. A., Bastow, I., Keir, D., Sparks, R., & Menand, T. (2014). Thermal models of dyke intrusion during development of continent-ocean transition. *Earth and Planetary Science Letters*, *385*, 145–153.

Davis, J., Bécel, A., & Buck, W. (2018). Estimating emplacement rates for seaward-dipping reflectors associated with the US East Coast Magnetic Anomaly. *Geophysical Journal International*, *215*(3), 1594–1603. https://doi.org/10.1093/gji/ggy360

Donnadieu, Y., Goddéris, Y., Pierrehumbert, R., Dromart, G., Fluteau, F., & Jacob, R. (2006). A GEOCLIM simulation of climatic and biogeochemical consequences of Pangea breakup. *Geochemistry, Geophysics, Geosystems*, *7*, Q11019. https://doi.org/10.1029/2006GC001278

Duff, P. D., & Kellogg, J. N. (2019). The Brunswick magnetic anomaly: Geophysical signature and geologic source. *Geology*, *47*(4), 355–358. https://doi.org/10.1130/g45462.1

Ebinger, C. (2005). Continental break-up: The East African perspective. *Astronomy & Geophysics*, *46*(2), 2.16–12.21.

Ebinger, C., & Casey, M. (2001). Continental breakup in magmatic provinces: An Ethiopian example. *Geology*, *29*(6), 527–530.

Ebinger, C. J., & Sleep, N. (1998). Cenozoic magmatism throughout East Africa resulting from impact of a single plume. *Nature*, *395*(6704), 788–791.

Eldholm, O., Gladczenko, T., Skogseid, J., & Planke, S. (2000). Atlantic volcanic margins: A comparative study. In A. Nøttvedt (Ed.), *Dynamics of the Norwegian Margin*, *Special Publications* (Vol. 167, pp. 411–428). London: Geological Society.

Eldholm, O., & Grue, K. (1994). North Atlantic volcanic margins: Dimensions and production rates. *Journal of Geophysical Research*, *99*(B2), 2955–2968. https://doi.org/10.1029/93JB02879

Eldholm, O., Skogseid, J., Planke, S., & Gladczenko, T. P. (1995). Volcanic margin concepts. In E. Banda, M. Torné, M. Talwani (Eds.), *Rifted ocean-continent boundaries* (pp. 1–16). Dordrecht, The Neatherlands: Springer.

Eldholm, O., Thiede, J., & Taylor, E. (1989). The Norwegian continental margin: Tectonic, volcanic, and paleoenvironmental framework. In O. Eldholm, et al. (Eds.), *Proceedings of the Ocean Drilling Program: Scientific results* (Vol. 104, pp. 5–25). Ocean Drilling Program: College Station, TX.

Franke, D. (2013). Rifting, lithosphere breakup and volcanism: Comparison of magma-poor and volcanic rifted margins. *Marine and Petroleum Geology*, *43*, 63–87.

Franke, D., Klitzke, P., Barckhausen, U., Berglar, K., Berndt, C., Damm, V., et al. (2019). Polyphase magmatism during the formation of the northern East Greenland continental margin. *Tectonics*, *38*, 2961–2982. https://doi.org/10.1029/2019TC005552

Franke, D., Ladage, S., Schnabel, M., Schreckenberger, B., Reichert, C., Hinz, K., et al. (2010). Birth of a volcanic margin off Argentina, South Atlantic. *Geochemistry, Geophysics, Geosystems*, *11*, Q0AB04. https://doi.org/10.1029/2009GC002715

Franke, D., Neben, S., Ladage, S., Schreckenberger, B., & Hinz, K. (2007). Margin segmentation and volcano-tectonic architecture along the volcanic margin off Argentina/Uruguay, South Atlantic. *Marine Geology*, *244*(1–4), 46–67.

Funck, T., Jackson, H. R., & Shimeld, J. (2011). The crustal structure of the Alpha Ridge at the transition to the Canadian Polar Margin: Results from a seismic refraction experiment. *Journal of Geophysical Research*, *116*, B12101. https://doi.org/10.1029/2011JB008411

Gallacher, R. J., Keir, D., Harmon, N., Stuart, G., Leroy, S., Hammond, J. O. S., et al. (2016). The initiation of segmented buoyancy-driven melting during continental breakup. *Nature Communications*, *7*(1), 1, 13110–9. https://doi.org/10.1038/ncomms13110

Gallahue, M., Stein, S., Stein, C. A., Jurdy, D., Barklage, M., & Rooney, T. (2020). A compilation of igneous rock volumes at volcanic passive continental margins from interpreted seismic profiles. *Marine and Petroleum Geology*, *122*. https://doi.org/10.1016/j.marpetgeo.2020.104635

Geoffroy, L. (2001). The structure of volcanic margins: Some problematics from the North-Atlantic/Labrador-Baffin system. *Marine and Petroleum Geology*, *18*(4), 463–469.

Geoffroy, L. (2005). Volcanic paddive margins. *Comptes Rendus Geoscience*, *337*, 1395–1408.

Geoffroy, L., Burov, E., & Werner, P. (2015). Volcanic passive margins: Another way to break up continents. *Scientific Reports*, *5*(1), 1–12. https://doi.org/10.1038/srep14828

Greene, J. A., Tominaga, M., Miller, N. C., Hutchinson, D. R., & Karl, M. R. (2017). Refining the formation and early evolution of the Eastern North American Margin: New insights from multiscale magnetic anomaly analyses. *Journal of Geophysical Research: Solid Earth*, *122*, 8724–8748. https://doi.org/10.1002/2017JB014308

Gupta, S., Kanna, N., & Akilan, A. (2017). Volcanic passive continental margin beneath Maitri station in central DML, East Antarctica: Constraints from crustal shear velocity through receiver function modelling. *Polar Research*, *36*(1), 1332947. https://doi.org/10.1080/17518369.2017.1332947

Hammond, J. O. S., Kendall, J. M., Stuart, G. W., Ebinger, C. J., Bastow, I. D., Keir, D., et al. (2013). Mantle upwelling and initiation of rift segmentation beneath the Afar Depression. *Geology*, *41*(6), 635–638. https://doi.org/10.1130/G33925.1

Hatcher, R. D. Jr. (2002). Alleghanian (Appalachian) orogeny, a product of zipper tectonics: Rotational transpressive continent-continent collision and closing of ancient oceans along irregular margins. In J. R. M. Catalan, R. D. Hatcher, Jr., R. Arenas, E. Díaz Garda (Eds.), *Variscan-Appalachian dynamics: The building of the late Paleozoic basement*, *Special Paper 364* (pp. 199–208). Boulder, CO, America: Geological Society.

Hatcher, R. D. Jr. (2010). The Appalachian orogen: A brief summary. In R. P. Tollo, M. J. Bartholomew, J. P. Hibbard, P. M. Karabinos (Eds.), *From Rodinia to Pangea: The lithotectonic record of the Appalachian re gion*, *Memoir* (Vol. 206, pp. 1–19). America: Geological Society. https://doi.org/10.1130/2010.1206(01)

Hayward, N., & Ebinger, C. (1996). Variations in the along-axis segmentation of the Afar Rift system. *Tectonics*, *15*(2), 244–257. https://doi.org/10.1029/95TC02292

Higgins, M. W., & Zietz, I. (1983). Geologic interpretation of geophysical maps of the pre-Cretaceous "basement" beneath the Coastal Plain of the southeastern United States. *Geological Society of America Memoirs*, *158*, 125–130.

Hinz, K. (1981). A hypothesis on terrestrial catastrophies wedges of very thick oceanward dipping layers beneath passive continental margins. Their origin and paleoenvironmental significance. *Geologisches Jahrbuch. Reihe E, Geophysik*, *22*, 3–28.

Holbrook, W., & Kelemen, P. (1993). Large igneous province on the US Atlantic margin and implications for magmatism during continental breakup. *Nature*, *364*(6436), 433–436.

Holbrook, W. S., Reiter, E. C., Purdy, G. M., Sawyer, D., Stoffa, P. L., Austin, J. A. Jr., et al. (1994). Deep structure of the US Atlantic continental margin, offshore South Carolina, from coincident ocean bottom and multichannel seismic data. *Journal of Geophysical Research*, *99*(B5), 9155–9178. https://doi.org/10.1029/93JB01821

Hopper, J. R., Mutter, J. C., Larson, R. L., & Mutter, C. Z. (1992). Magmatism and rift margin evolution: Evidence from northwest Australia. *Geology*, *20*(9), 853–857. https://doi.org/10.1130/0091-7613(1992)020<0853:marmee>2.3.co;2

Hutchinson, D. R., Grow, J. A., Klitgord, K. D., & Swift, B. A. (1982). Deep structure and evolution of the Carolina Trough. In J. S. Watkins, & C. L. Drake (Eds.), *Studies in continental margin geology* (Vol. 34, pp. 129–152). America: American Association of Petroleum Geologists.

Hutchinson, D. R., Poag, C. W., & Popenoe, P. (1995). Geophysical database of the east coast of the United States; southern Atlantic margin, stratigraphy and velocity from multichannel seismic profiles. *U.S.* Geological Survey Open-File Report 95–27.

Keen, C., & Potter, D. (1995). The transition from a volcanic to a nonvolcanic rifted margin off eastern Canada. *Tectonics*, *14*(2), 359–371. https://doi.org/10.1029/94TC03090

Keir, D., Bastow, I. D., Corti, G., Mazzarini, F., & Rooney, T. O. (2015). The origin of along-rift variations in faulting and magmatism in the Ethiopian Rift. *Tectonics*, *34*, 464–477. https://doi.org/10.1002/2014TC003698

Keir, D., Bastow, I. D., Pagli, C., & Chambers, E. L. (2013). The development of extension and magmatism in the Red Sea rift of Afar. *Tectonophysics*, *607*, 98–114. https://doi.org/10.1016/j.tecto.2012.10.015

Kelemen, P. B., & Holbrook, W. S. (1995). Origin of thick, high-velocity igneous crust along the US East Coast Margin. *Journal of Geophysical Research*, *100*(B6), 10,077–10,094. https://doi.org/10.1029/95JB00924

Keller, F. Jr., Meuschke, J., & Alldredge, L. (1954). Aeromagnetic surveys in the Aleutian, Marshall, and Bermuda islands. *Eos, Transactions American Geophysical Union*, *35*(4), 558–572.

Kendall, J. M., Stuart, G. W., Ebinger, C. J., Bastow, I. D., & Keir, D. (2005). Magma-assisted rifting in Ethiopia. *Nature*, *433*(7022), 146–148. https://doi.org/10.1038/nature03161

Keranen, K., Klemperer, S., Gloaguen, R., & Group, E. W. (2004). Three-dimensional seismic imaging of a protoridge axis in the Main Ethiopian rift. *Geology*, *32*(11), 949–952.

Klingelhoefer, F., Labails, C., Cosquer, E., Rouzo, S., Géli, L., Aslanian, D., et al. (2009). Crustal structure of the SW-Moroccan margin from wide-angle and reflection seismic data (the DAKHLA experiment) Part A: Wide-angle seismic models. *Tectonophysics*, *468*(1–4), 63–82. https://doi.org/10.1016/j.tecto.2008.07.022

Klitgord, K., & Berhrendt, J. C. (1979). Basin structure of the U.S. Atlantic margin. In L. M. S. Watkins & P. W. Dickerson (Eds.), *Geological and geophysical investigations of continental margin* (pp. 85–112). Boulder, CO: Geological Society of America.

Klitgord, K., & Schouten, H. (1986). Plate kinematics of the central Atlantic. In P. R. Vogt & B. E. Tucholke (Eds.), *The geology of North America, Vol. M, the western North Atlantic region* (pp. 351–378). Geological Society of America: Boulder, CO.

Klitgord, K. D., Hutchinson, D. R., & Schouten, H. (1988). U.S. Atlantic continental margin: Structural and tectonic framework. In R. E. Sheridan & J. A. Grow (Eds.), *The geology of North America, I-2, the Atlantic Continental Margin, US* (pp. 19–55). Geological Society of America: Boulder, CO.

Klitgord, K. D., Poag, C., Schneider, C., & North, L. (1994). Geophysical database of the East Coast of the United States northern Atlantic margin-cross sections and gridded database (Georges Bank Basin, Long Island Platform, and Baltimore Canyon Trough). *U.S. Geological Survey Open-File Report 94–637*.

Koopmann, H., Franke, D., Schreckenberger, B., Schulz, H., Hartwig, A., Stollhofen, H., & di Primio, R. (2014). Segmentation and volcano-tectonic characteristics along the SW African continental margin, South Atlantic, as derived from multichannel seismic and potential field data. *Marine and Petroleum Geology*, *50*, 22–39.

Labails, C., Olivet, J.-L., Aslanian, D., & Roest, W. R. (2010). An alternative early opening scenario for the Central Atlantic Ocean. *Earth and Planetary Science Letters*, *297*(3–4), 355–368.

Labails, C., Olivet, J.-L., & the Dakhla study group (2009). Crustal structure of the SW Moroccan margin from wide-angle and reflection seismic data (the Dakhla experiment). Part B—The tectonic heritage. *Tectonophysics*, *468*, 83–97. https://doi.org/10.1016/j.tecto.2008.08.028

Lase Study Group (1986). Deep structure of the US East Coast passive margin from large aperture seismic experiments (LASE). *Marine and Petroleum Geology*, *3*(3), 234–242. https://doi.org/10.1016/0264-8172(86)90047-4

Lefort, J., & Max, M. (1991). Is there an Archean crust beneath Chesapeake Bay? *Tectonics*, *10*(1), 213–226. https://doi.org/10.1029/90TC00911

Li, C. F., Lu, Y., & Wang, J. (2017). A global reference model of Curie-point depths based on EMAG2. *Scientific Reports*, *7*(1), 1–9. https://doi.org/10.1038/srep45129

Lin, J., Purdy, G., Schouten, H., Sempere, J.-C., & Zervas, C. (1990). Evidence from gravity data for focused magmatic accretion along the Mid-Atlantic Ridge. *Nature*, *344*(6267), 627–632. https://doi.org/10.1038/344627a0

Lizarralde, D., Axen, G. J., Brown, H. E., Fletcher, J. M., González-Fernández, A., Harding, A. J., et al. (2007). Variation in styles of rifting in the Gulf of California. *Nature*, *448*(7152), 466–469. https://doi.org/10.1038/nature06035

Lizarralde, D., Holbrook, W. S., & Oh, J. (1994). Crustal structure across the Brunswick magnetic anomaly, offshore Georgia, from coincident ocean bottom and multi-channel seismic data. *Journal of Geophysical Research*, *99*(B11), 21,741–21,757. https://doi.org/10.1029/94JB01550

Lowell, J. D., & Genik, G. J. (1972). Sea-floor spreading and structural evolution of Southern Red Sea. *American Association of Petroleum Geologists Bulletin*, *56*, 247–259.

Lowrie, W. (2007). *Fundamentals of geophysics*. New York, USA: Cambridge University Press.

Lynner, C., J. A. van Avendonk, H., Bécel, A., Christeson, G. L., Dugan, B., Gaherty, J. B., et al. (2020). The eastern North American margin community seismic experiment: An amphibious active-and passive-source dataset. *Seismological Research Letters*, *91*(1), 533–540. https://doi.org/10.1785/0220190142

Magde, L. S., & Sparks, D. W. (1997). Three-dimensional mantle upwelling, melt generation, and melt migration beneath segment slow spreading ridges. *Journal of Geophysical Research*, *102*(B9), 20,571–20,583. https://doi.org/10.1029/97jb01278

Makris, J., & Ginzburg, A. (1987). The Afar Depression: Transition between continental rifting and sea-floor spreading. *Tectonophysics*, *141*(1–3), 199–214.

Manighetti, I., Tapponnier, P., Courtillot, V., Gruszow, S., & Gillot, P. Y. (1997). Propagation of rifting along the Arabian-Somalia plate boundary: The Gulfs of Aden and Tadjoura. *Journal of Geophysical Research*, *102*(B2), 2681–2710.

Manighetti, I., Tapponnier, P., & Gallet, Y. (2001). Strain transfer between disconnected, propagating rifts in Afar. *Journal of Geophysical Research*, *106*(B7), 13,613–13,665.

Manighetti, I., Tapponnier, P., Gillot, P. Y., Jacques, E., Courtillot, V., Armijo, R., et al. (1998). Propagation of rifting along the Arabia-Somalia plate boundary: Into Afar. *Journal of Geophysical Research*, *103*(B3), 4947–4974.

Mann, P., Gahagan, L., & Gordon, M. B. (2003). Tectonic setting of the world's giant oil and gas fields. *Giant oil and gas fields of the decade, 1990–1999*, 15–105.

Manspeizer, W., & Cousminer, H. L. (1988). Late Triassic-Early Jurassic synrift basins of the US Atlantic margin. In R. E. Sheridan & J. A. Grow (Eds.), *The geology of North America, I-2, the Atlantic Continental Margin, U. S* (pp. 197–216). Geological Society of America: Boulder, CO.

Marzen, R. E., Shillington, D. J., Lizarralde, D., & Harder, S. H. (2019). Constraints on Appalachian orogenesis and continental rifting in the southeastern United States from wide-angle seismic data. *Journal of Geophysical Research: Solid Earth*, *124*, 6625–6652. https://doi.org/10.1029/2019JB017611

Marzoli, A., Callegaro, S., Dal Corso, J., Davies, J. H., Chiaradia, M., Youbi, N., et al. (2018). The Central Atlantic magmatic province (CAMP): A review. In L. Tanner (Ed.), *The Late Triassic World* (pp. 91–125). Basel, Switzerland: Springer.

McBride, J., & Nelson, K. (1988). Integration of COCORP deep reflection and magnetic anomaly analysis in the southeastern United States: Implications for origin of the Brunswick and East Coast magnetic anomalies. *Geological Society of America Bulletin*, *100*(3), 436–445.

McHone, J. G. (2000). Non-plume magmatism and rifting during the opening of the central Atlantic Ocean. *Tectonophysics*, *316*(3–4), 287–296.

Menzies, M. A., Klemperer, S. L., Ebinger, C. J., & Baker, J. (2002). Characteristics of volcanic rifted margins. In M. A. Menzies, S. L. Klemperer, C. J. Ebinger, J. Baker (Eds.), *Volcanic rifted margins*, *Special Paper 362* (pp. 1–14). Boulder, CO: Geological Society of America.

Mjelde, R., Kvarven, T., Faleide, J. I., & Thybo, H. (2016). Lower crustal high-velocity bodies along North Atlantic passive margins, and their link to Caledonian suture zone eclogites and Early Cenozoic magmatism. *Tectonophysics*, *670*, 16–29. https://doi.org/10.1016/j.tecto.2015.11.021

Monteleone, V., Minshull, T. A., & Marin-Moreno, H. (2019). Spatial and temporal evolution of rifting and continental breakup in the Eastern Black Sea Basin revealed by long-offset seismic reflection data. *Tectonics*, *38*, 2646–2667. https://doi.org/10.1029/2019TC005523

Morgan, R., & Watts, A. (2018). Seismic and gravity constraints on flexural models for the origin of seaward dipping reflectors. *Geophysical Journal International*, *214*(3), 2073–2083. https://doi.org/10.1093/gji/ggy243

Müller, R. D., Sdrolias, M., Gaina, C., & Roest, W. R. (2008). Age, spreading rates, and spreading asymmetry of the world's ocean crust. *Geochemistry, Geophysics, Geosystems*, *9*, Q04006. https://doi.org/10.1029/2007GC001743

Mutter, J. C. (1985). Seaward dipping reflectors and the continent-ocean boundary at passive continental margins. *Tectonophysics*, *114*(1–4), 117–131.

Mutter, J. C., Talwani, M., & Stoffa, P. L. (1982). Origin of seaward-dipping reflectors in oceanic crust off the Norwegian margin by "subaerial sea-floor spreading". *Geology*, *10*(7), 353–357. https://doi.org/10.1130/0091-7613(1982)10<353:oosrio>2.0.co;2

Nelson, R., Patton, T., & Morley, C. (1992). Rift-segment interaction and its relation to hydrocarbon exploration in continental rift systems (1). *AAPG Bulletin*, *76*(8), 1153–1169.

Nomade, S., Knight, K. B., Beutel, E., Renne, P. R., Verati, C., Féraud, G., et al. (2007). Chronology of the Central Atlantic Magmatic Province: Implications for the Central Atlantic rifting processes and the Triassic-Jurassic biotic crisis. *Palaeogeography, Palaeoclimatology, Palaeoecology*, *244*(1–4), 326–344. https://doi.org/10.1016/j.palaeo.2006.06.034

Oh, J., Austin, J. A. Jr., Phillips, J. D., Coffin, M., & Stoffa, P. L. (1995). Seaward-dipping reflectors offshore the southeastern United States: Seismic evidence for extensive volcanism accompanying sequential formation of the Carolina Trough and Blake Plateau Basin. *Geology*, *23*, 9–12. https://doi.org/10.1130/0091-7613(1995)023<0009:SDROTS>2.3.CO;2

Pariso, J. E., & Johnson, H. P. (1991). Alteration processes at deep sea drilling project/ocean drilling program hole 504B at the Costa Rica rift: Implications for magnetization of oceanic crust. *Journal of Geophysical Research*, *96*(B7), 11,703–11,722. https://doi.org/10.1029/91JB00872

Parker, E. Jr. (2014). Crustal magnetism, tectonic inheritance, and continental rifting in the southeastern United States. *GSA Today*, *24*(4), 4–9.

Parker, R. (1973). The rapid calculation of potential anomalies. *Geophysical Journal International*, *31*(4), 447–455.

Parker, R., & Huestis, S. (1974). The inversion of magnetic anomalies in the presence of topography. *Journal of Geophysical Research*, *79*(11), 1587–1593. https://doi.org/10.1029/JB079i011p01587

Péron-Pinvidic, G., Manatschal, G., & Osmundsen, P. T. (2013). Structural comparison of archetypal Atlantic rifted margins: A review of observations and concepts. *Marine and Petroleum Geology*, *43*, 21–47. https://doi.org/10.1016/j.marpetgeo.2013.02.002

Pollack, H. N., Hurter, S. J., & Johnson, J. R. (1993). Heat flow from the Earth's interior: Analysis of the global data set. *Reviews of Geophysics*, *31*(3), 267–280.

Rajaram, M. (2007). Depth to Curie temperature. In D. Gubbins & E. Herrero-Bervera (Eds.), *Encyclopedia of geomagnetism and paleomagnetism* (pp. 157–158). Dordrecht, The Neatherlands: Springer.

Rankin, D. W. (1994). Continental margin of the eastern United States: Past and present. In R. C. Speed (Ed.), *Phanerozoic evolution of North America continent-ocean transitions* (pp. 129–218). Boulder, CO: Geological Society of America.

Roeser, H. A., Steiner, C., Schreckenberger, B., & Block, M. (2002). Structural development of the Jurassic magnetic quiet zone off Morocco and identification of middle Jurassic magnetic lineations. *Journal of Geophysical Research*, *107*(B10), 2207. https://doi.org/10.1029/2000JB000094

Schettino, A., & Turco, E. (2009). Breakup of Pangaea and plate kinematics of the central Atlantic and Atlas regions. *Geophysical Journal International*, *178*(2), 1078–1097. https://doi.org/10.1111/j.1365-246X.2009.04186.x

Schlische, R. W. (1993). Anatomy and evolution of the Triassic-Jurassic continental rift system, eastern North America. *Tectonics*, *12*(4), 1026–1042. https://doi.org/10.1029/93TC01062

Schlische, R. W., Withjack, M. O., & Olsen, P. E. (2003). Relative timing of CAMP, rifting, continental breakup, and basin inversion: Tectonic significance. In W. E. Hames, J. G. Mchone, P. Renne, C. Ruppel (Eds.), *The Central Atlantic Magmatic Province: Insights from fragments of Pangea, Geophysical Monograph Series* (Vol. 136, pp. 33–59). Washington, DC: American Geophysical Union.

Schouten, H., Klitgord, K. D., & Whitehead, J. A. (1985). Segmentation of mid-ocean ridges. *Nature*, *317*(6034), 225–229. https://doi.org/10.1038/317225a0

Sempéré, J.-C., Lin, J., Brown, H. S., Schouten, H., & Purdy, G. (1993). Segmentation and morphotectonic variations along a slow-spreading center: The Mid-Atlantic Ridge (24°00′N–30°40′N). *Marine Geophysical Researches*, *15*(3), 153–200.

Sheridan, R. E. (1989). The Atlantic passive margin. In A. W. Bally, & A. R. Palmer (Eds.), *The geology of North America: An overview, U. S* (pp. 81–96). Geological Society of America: Boulder, CO.

Sheridan, R. E., Maguire, T. J., Feigenson, M. D., Patino, L. C., & Volkert, R. A. (1999). Grenville age of basement rocks in Cape May NJ well new evidence for Laurentian crust in U.S. Atlantic Coastal Plain basement Chesapeake terrane. *Geodynamics Series*, *27*, 623–633.

Sheridan, R. E., Musser, D. L., Glover, L. III, Talwani, M., Ewing, J. I., Holbrook, W. S., et al. (1993). Deep seismic reflection data of EDGE US mid-Atlantic continental-margin experiment: Implications for Appalachian sutures and Mesozoic rifting and magmatic underplating. *Geology*, *21*(6), 563–567. https://doi.org/10.1130/0091-7613(1993)021<0563:DSRDOE>2.3.CO;2

Shillington, D. J., Holbrook, W. S., van Avendonk, H. J. A., Tucholke, B. E., Hopper, J. R., Louden, K. E., et al. (2006). Evidence for asymmetric nonvolcanic rifting and slow incipient oceanic accretion from seismic reflection data on the Newfoundland margin. *Journal of Geophysical Research*, *111*, B09402. https://doi.org/10.1029/2005JB003981

Shillington, D. J., Scott, C. L., Minshull, T. A., Edwards, R. A., Brown, P. J., & White, N. (2009). Abrupt transition from magma-starved to magma-rich rifting in the eastern Black Sea. *Geology*, *37*(1), 7–10. https://doi.org/10.1130/g25302a.1

Shuck, B. D., van Avendonk, H. J., & Bécel, A. (2019). The role of mantle melts in the transition from rifting to seafloor spreading offshore eastern North America. *Earth and Planetary Science Letters*, *525*, 115,756. https://doi.org/10.1016/j.epsl.2019.115756

Simms, M. J., & Ruffell, A. H. (1989). Synchroneity of climatic change and extinctions in the Late Triassic. *Geology*, *17*(3), 265–268.

Talwani, M., & Abreu, V. (2000). Inferences regarding initiation of oceanic crust formation from the US East Coast margin and conjugate South Atlantic margins. *Geophysical Monograph Series*, *115*, 211–234.

Talwani, M., Ewing, J., Sheridan, R. E., Holbrook, W. S., & Glover, L. (1995). The EDGE experiment and the US East Coast magnetic anomaly. In E. Banda, M. Torné, M. Talwani (Eds.), *Rifted ocean-continent boundaries* (pp. 155–181). Dordrecht, The Netherlands: Springer.

Taylor, P. T., Zietz, I., & Dennis, L. S. (1968). Geologic implications of aeromagnetic data for the eastern continental margin of the United States. *Geophysics*, *33*(5), 775–780.

Thomas, W. A. (2019). Tectonic inheritance at multiple scales during more than two complete Wilson cycles recorded in eastern North America. In R. W. Wilson, G. A. Houseman, K. J. W. McCaffrey, A. G. Doré, S. J. H. Butter (Eds.), *Fifty years of the Wilson cycle concept in plate tectonics*, *Special Publications* (Vol. 470, pp. 337–352). London: Geological Society.

Tréhu, A. M., Ballard, A., Dorman, L., Gettrust, J., Klitgord, K. D., & Schreiner, A. (1989). Structure of the lower crust beneath the Carolina Trough, US Atlantic continental margin. *Journal of Geophysical Research*, *94*(B8), 10,585–10,600. https://doi.org/10.1029/JB094iB08p10585

Tugend, J., Gillard, M., Manatschal, G., Nirrengarten, M., Harkin, C., Epin, M. E., et al. (2018). Reappraisal of the magma-rich versus magma-poor rifted margin archetypes. In K. R. McClay & J. A. Hammerstein (Eds.), *Passive margins: Tectonics, sedimentation and magmatism*, *Special Publications* (Vol. 476, pp. 23–47). London: Geological Society.

Van Avendonk, H. J., Holbrook, W. S., Nunes, G. T., Shillington, D. J., Tucholke, B. E., Louden, K. E., et al. (2006). Seismic velocity structure of the rifted margin of the eastern Grand Banks of Newfoundland, Canada. *Journal of Geophysical Research*, *111*, B11404. https://doi.org/10.1029/2005JB004156

Vandamme, D., & Ali, J. R. (1998). 21. Paleomagnetic results from basement rocks from Site 917 (East Greenland Margin). In A. D. Saunders, H. C. Larsen, S. W. Wise, Jr. (Eds.), *Proceedings of the Ocean Drilling Program: Scientific results* (Vol. 152, p. 259–264). Ocean Drilling Program: College Station, TX.

Vogt, P. (1973). Early events in the opening of the North Atlantic. In D. H. Taling & S. K. Runcorn (Eds.), *Implications of continental rift to the Earth sciences* (Vol. 2, pp. 693–712). New York: Academic Press.

Wang, Y., Forsyth, D. W., & Savage, B. (2009). Convective upwelling in the mantle beneath the Gulf of California. *Nature*, *462*(7272), 499–501. https://doi.org/10.1038/nature08552

Weiwei, D., Schnabel, M., Franke, D., Aiguo, R., & Zhenli, W. (2012). Crustal structure across the northwestern margin of South China Sea: Evidence for magma-poor rifting from a wide-angle seismic profile. *Acta Geologica Sinica-English Edition*, *86*(4), 854–866.

White, R., & McKenzie, D. (1989). Magmatism at rift zones: The generation of volcanic continental margins and flood basalts. *Journal of Geophysical Research*, *94*(B6), 7685–7729. https://doi.org/10.1029/jb094ib06p07685

White, R. S., Smith, L. K., Roberts, A. W., Christie, P. A. F., & Kusznir, N. J. (2008). Lower-crustal intrusion on the North Atlantic continental margin. *Nature*, *452*(7186), 460–464. https://doi.org/10.1038/nature06687

White, R. S., Spence, G. D., Fowler, S. R., McKenzie, D. P., Westbrook, G. K., & Bowen, A. N. (1987). Magmatism at rifted continental margins. *Nature*, *330*(6147), 439–444.

Whitehead, J. A., Dick, H. J., & Schouten, H. (1984). A mechanism for magmatic accretion under spreading centres. *Nature*, *312*(5990), 146–148. https://doi.org/10.1038/312146a0

Whitmarsh, R. B., Manatschal, G., & Minshull, T. A. (2001). Evolution of magma-poor continental margins from rifting to seafloor spreading. *Nature*, *413*(6852), 150–154. https://doi.org/10.1038/35093085

Wilson, J. T. (1966). Did the Atlantic close and then re-open? *Nature*, *211*(5050), 676–681. https://doi.org/10.1038/211676a0

Wilson, M. (1997). Thermal evolution of the Central Atlantic passive margins: Continental break-up above a Mesozoic super-plume. *Journal of the Geological Society*, *154*(3), 491–495.

Withjack, M. O., Schlische, R. W., & Olsen, P. E. (1998). Diachronous rifting, drifting, and inversion on the passive margin of central eastern North America: An analog for other passive margins. *AAPG Bulletin*, *82*(5), 817–835.

Withjack, M. O., Schlische, R. W., & Olsen, P. E. (2012). Development of the passive margin of eastern North America: Mesozoic rifting, igneous activity, and breakup. In D. G. Roberts & A. W. Bally (Eds.), *Regional geology and tectonics: Phanerozoic rift systems and sedimentary basins* (Vol. 1, pp. 301–335). Amsterdam, The Neatherlands: Elsevier.

References From the Supporting Information

Robertson, E. C. (1988). Thermal properties of rocks. *U.S.* Geological Survey Open-File Report *88–441*.

Sleep, N. H., & Fujita, K. (1997). *Principles of geophysics*. Malden, Massachusetts: Blackwell Science.